Ribosomal RNA synthesis by RNA polymerase I is subject to premature termination of transcription.

Chaïma Azouzi[1], Katrin Schwank[2], Sophie Queille[1], Marta Kwapisz[1], Marion Aguirrebengoa[3], Anthony Henras[2], Simon Lebaron[1], Herbert Tschochner[2], Annick Lesne[4], Frédéric Beckouët[1], Olivier Gadal[1*] and Christophe Dez[1*]

1: Molecular, Cellular and Developmental Biology Unit (MCD), Centre de Biologie Intégrative (CBI), Université de Toulouse, CNRS, UPS, 31062 Toulouse, France.

2: Universität Regensburg, Regensburg Center of Biochemistry (RCB), Lehrstuhl Biochemie III, Regensburg, Germany.

3: Centre de Biologie Intégrative (CBI), Université de Toulouse, CNRS, UPS, 31062 Toulouse, France.

4: Laboratoire de Physique Théorique de la Matière Condensée (LPTMC), Sorbonne Université, Paris, France

* co-Corresponding author:

Christophe Dez

email: christophe.dez@univ-tlse3.fr

Phone: +33(0)5 61 33 59 39; Fax: +33 (0)5 61 33 58 86;

Olivier Gadal

email: olivier.gadal@ univ-tlse3.fr

Phone: +33(0)5 61 33 59 39; Fax: +33 (0)5 61 33 58 86;

Keywords : yeast, rRNA transcription, RNA Polymerase I, Premature Termination of Transcription (PTT), BMH21.

ABSTRACT

The RNA polymerase I (Pol I) enzyme that synthesizes large rRNA precursors, exhibits high rate of pauses during elongation, indicative of a discontinuous process. We show here that Premature Termination of Transcription (PTT) by Pol I is a critical regulatory step limiting rRNA production *in vivo*. The Pol I mutant, SuperPol (RPA135-F301S), produces 1.5-fold more rRNA than the wild type (WT). Combined CRAC and rRNA analysis link increased rRNA production in SuperPol to reduced PTT, resulting in shifting polymerase distribution toward the 3' end of rDNA genes. *In vitro*, SuperPol shows reduced nascent transcript cleavage, associated with more efficient transcript elongation after pauses, to the detriment of transcriptional fidelity. Notably, SuperPol is resistant to BMH-21, a drug impairing Pol I elongation and inducing proteasome-mediated degradation of Pol I subunits. Compared to WT, SuperPol maintains subunit stability and sustains high transcription levels upon BMH-21 treatment. These comparative results show that PTT is alleviated in SuperPol while it is stimulated by BMH-21 in WT Pol I.

INTRODUCTION

Ribosome biogenesis is a major energy consuming process in exponentially growing cells. In eukaryotes, making a ribosome requires the coordinate activities of the three eukaryotic nuclear RNA polymerases, accounting for up to 75% of total cellular transcriptional activity (Warner, 1999). Half of all RNA polymerase II (Pol II) initiation events are devoted to the production of mRNAs encoding ribosomal proteins and ribosome biogenesis factors. Furthermore, a prodigious amount of ribosomal RNAs (rRNAs) is synthesized by the combined transcriptional activity of the RNA Polymerase I (Pol I), which leads to the production the three large rRNAs, namely 18S, 5.8S and 25S rRNAs, as well as the RNA polymerase III (Pol III), which synthesizes the 5S rRNA. In the yeast *Saccharomyces cerevisiae*, the first step of the ribosome assembly process is the production of 35S rRNA (corresponding to 47S in human) by Pol I. Up to hundreds of Pol I enzymes can simultaneously transcribe a single rDNA gene. During Pol I transcription, nascent 35S pre-rRNA is folded and assembled with ribosomal proteins into large pre-ribosomes by several ribosome biogenesis factors. Within pre-ribosomes, rRNAs are co-transcriptionally matured by endonucleolytic cleavages and exonucleolytic trimming (Henras et al., 2015; Kos and Tollervey, 2010; Woolford and Baserga, 2013). A huge amount of cell resources is invested in ribosome production, making its regulation crucial for cell homeostasis. Importantly, the production and assembly of nearly 80 ribosomal proteins with four different rRNAs imposes regulatory challenges that must be adapted to fluctuating environmental conditions. To cope with such massive production, Pol I activity should be highly regulated. Miller chromatin spreads, allowing single molecule analysis of the rDNA gene transcribed by Pol I, clearly demonstrates the exceptional efficiency of transcription initiation by Pol I in ideal growth conditions (Albert et al., 2011). In fact, such initiation level leads to almost 50% occupancy of Pol I along the length of the rDNA (French et al., 2003).

In both yeast and mammals, essential factors required for Pol I initiation were identified through genetic and biochemical approaches (Grummt, 2003; Moss et al., 2007). The structures of Pol I initiation complex (Pre-Initiation Complex and Initially Transcribing Complex) are now available (Engel et al., 2018). Although Pol I transcription is well known to be regulatable at the initiation level (Blattner

et al., 2011; Sadian et al., 2019; Schneider et al., 2007), rRNA synthesis and pre-rRNA processing are, at least partially, controlled during the elongation phase of Pol I transcription (Azouzi et al., 2021; Schneider et al., 2007). A statistical view of Pol I pausing within rDNA was obtained using high-throughput methods such as Net-Seq or CRAC (Clarke et al., 2018; Turowski et al., 2020). Similar to other RNA polymerases, the Pol I elongation process is based on Brownian ratchet in which energy-driven mechanism favors forward rather than backward steps. As reported by several studies, Pol I is prone to frequent pausing events and/or regions with slower elongation rates possibly accompanied by backtracking (Clarke et al., 2018; Dangkulwanich et al., 2013; Duval et al., 2023; Guajardo and Sousa, 1997; Scull et al., 2020; Turowski et al., 2020). The dynamic of Pol I elongation is influenced by various factors, such as the folding of the nascent rRNA as well as the supercoiling of the rDNA template, as shown by biophysical modeling recapitulating Pol I density along the gene (Kim et al., 2019; Lesne et al., 2018; Liu and Wang, 1987; Turowski et al., 2020). This pausing pattern results in a strong accumulation of Pol I elongation complex in the 5' end of the rDNA gene. The high density of polymerases in the 5' ETS region is also correlated with major early pre-rRNA assembly events occurring in the 5' region of nascent rRNA (Chaker-Margot et al., 2017). Another area of high Pol I density on the rDNA can be observed between the 18S and 25S rRNA genes. These areas of high pausing frequency also correspond to a crucial co-transcriptional assembly event, leading to the completion of the small ribosomal subunit rRNA precursor (20S pre-rRNA), and the production of the rRNA molecules composing the large ribosomal subunit (5.8S and 25S). Such pausing patterns correlate with major pre-ribosome assembly steps and also suggest a high level of optimization of Pol I activity.

Using genetic tools, we could show that wild-type Pol I transcriptional activity, which is the highest among the three nuclear RNA polymerases, can be further increased. We recently identified Pol I mutant bearing a single amino acid substitution on the second largest subunit: *RPA135-F301S* allele (Darrière et al., 2019), hereafter named SuperPol. This mutant was isolated as an extragenic suppressor of growth defect of Pol I mutant lacking subunits Rpa49 (orthologs of human PAF53). This mutation increases rRNA production in yeast, measured by transcriptional run-on. Surprisingly, using

either Miller spread or ChIP techniques, we were unable to detect any significant variation in the loading rate of Pol I on rDNA in the mutant compared to the wild-type. Importantly, an accumulation of 35S rRNA in cells bearing SuperPol was only observed in absence of Rrp6, the nuclear component of the exosome that is involved in rRNA decay (Darrière et al., 2019).

In this study, we first set up a technique we called Pol I Transcriptional Monitoring Assay (TMA) to confirm a 50% increase of rRNA synthesis in SuperPol relative to wild-type background in living cells. We used CRAC method to demonstrate that the SuperPol mutant is prone to fewer stalling events in the 5' end of the gene, compared to a WT Pol I. This modified pausing pattern correlates with a decreased premature termination of the transcription (PTT) for SuperPol relative to wild-type Pol I. This decreased premature termination of transcription results in a global shift of the elongation complexes toward the 3’ end of the gene. This suggests an increased processivity of the mutant, allowing for greater production of full-length 35S rRNA compared to the WT. Using purified WT Pol I and SuperPol *in vitro*, we observed a modified cleavage pattern on artificial templates. This modified activity is associated with more efficient transcript elongation after pausing, at the expense of transcriptional fidelity for SuperPol compared to WT Pol I.

Finally, we demonstrated that SuperPol is resistant to the drug BMH-21, which is known to be a poison for Pol I elongation (Colis et al., 2014; Jacobs et al., 2022; Peltonen et al., 2014a, 2014b; Wei et al., 2018). We could show that BMH-21 strongly promote Pol I PTT. Altogether, these results suggest that Pol I can be regulated by PTT, and that BMH-21 targets stalled/paused Pol I and stimulates their premature termination *in vivo*.

MATERIAL AND METHODS

Strains, media, plasmids and cloning

Propagation of yeast was performed using standard rich YP medium (1% yeast extract, 2% peptone) supplemented with either 2% glucose (YPD) or 2% galactose (YPG) or using minimal YNB medium (0.67% yeast nitrogen base, 0.5% (NH4)2SO4 and 2% glucose or galactose) supplemented with the required amino acids. Yeast strains used in this study were derivatives of *S. cerevisiae* BY4741, originating from the S288C background. Strains 3207 and 3208 were constructed as follows: a PCR cassette containing the HTP-tag sequence followed by the kanamycin resistance (kanR) selectable marker, was amplified by PCR from the plasmid pBS-1539-HTP (S Granneman et al., 2009) using primers 1898 and 1899. The PCR fragment was inserted by homologous recombination downstream of the RPA135 and RPC128 chromosomal open reading frame in the BY4742 strain. Transformants were selected for uracil prototrophy, screened by immunoblotting and sequenced. Deletion of *RRP6* was performed as previously described (Dez et al., 2006).

Pol I TMA

Yeast cells were grown in phosphate depleted YPD medium (Briand et al., 2001) to an OD600 of 0.8 at 30°C. The RNAs were labeled in vivo by incubation of 1ml culture aliquots with 150 µCi [32P]orthophosphate (P-RB-1, (54mCi/ml) Hartmann Analytic, Braunschweig, Germany) for the indicated time. Cells were collected by centrifugation and the pellets were frozen in liquid nitrogen. RNAs were then extracted (Beltrame and Tollervey, 1992) and precipitated with ethanol. Slot blot were loaded with single-stranded 80-mers DNA oligonucleotides: 1855 (NTS2), 1856 (5'ETS-1), 1857 (5'ETS-2), 1858 (5'ETS-3), 1859 (18S.2), 1860 (25S.1), 1861 (3'ETS), 1863 (5S US) and 1864 (5S DS) and hybridization was performed as previously described for transcription run-on (Prescott et al., 2004; Wery et al., 2009).

Western analyses

Proteins from total extracts obtained after TCA precipitation or from immunoprecipitated pellets, were separated on 4-12 % polyacrylamide/SDS gels (Biorad) and transferred to Hybond-ECL membranes (GE Healthcare). HTP-tagged proteins were detected using rabbit PAP (Sigma) diluted 10,000 fold. Pol I subunits were detected using poly clonal anti-PoI I total antibody as previously described (Riva et al., 1982). Swi6 was detected using polyclonal anti-Swi6 antibody (Cusabio, PA362844XA01SVG).

RNA extractions and Northern Hybridizations

RNA extractions and Northern hybridizations were performed as previously described (Beltrame and Tollervey, 1992). Low molecular weight RNA products were resolved on 8% Polyacrylamide/8.3M urea gels.

CRAC experiment

Samples were processed as previously described (Turowski et al., 2020)

Culture:

Yeast cells expressing Rpa135 and/or Rpc128 fused at the C-terminus to the tripartite HTP tag (His6 tag-TEV protease cleavage site-Protein A tag) and the wild-type BY4741 strain (negative control) were grown at 30 °C in 2.5 L of synthetic dextrose (SD) medium with 2% glucose, lacking tryptophan, to an OD600 of 0.9. When indicated, 35µM of BMH-21 were added to the culture for 15 min before UV irradiation.

UV crosslinking, cell lysis, supernatant clarification:

Cells were irradiated with a megatron for 100 sec with UV light at 254 nm and harvested. Cells were resuspended in TNMC100 buffer (50 mM Tris-HCl pH 7.5, 150 mM NaCl, 0.1% NP-40, 5 mM $MgCl_2$, 10 mM $CaCl_2$, 5mM β-mercaptoethanol, 50U of DNase RQ1 and a protease-inhibitor cocktail - 1 tablet/50 mL) and lysed by mechanical disruption using zirconia beads with six one-minute pulses, with cooling on ice in between. The supernatant was spun for 20 minutes at 13000 rpm.

IgG sepharose incubation + washes +TEV elution:

Cell lysates were mixed with 400 µl IgG SepharoseTM 6 Fast Flow slurry (GE Healthcare) pre-equilibrated with TNM100 buffer (50 mM Tris-HCl pH 7.8, 100 mM NaCl, 0.1% NP-40, 5 mM MgCl2, 5mM β-mercaptoethanol) and incubated for two hours at 4 °C on a stirring wheel. Beads were washed two times with TNM600 buffer (50 mM Tris-HCl pH 7.8, 600 mM NaCl, 1.5 mM $MgCl_2$, 0.1% NP-40, 5 mM β-mercaptoethanol) and two times with TNM100 buffer, then resuspended in 600 µl TNM100 buffer and transferred into Micro Bio-Spin 6 columns (Bio-Rad). The elution from IgG Sepharose beads was achieved by incubation with 30 µl homemade GST-tagged TEV protease for two hours on a shaking table at 16 °C.

Digestion of TEV eluates + Ni-NTA incubation + washes:

TEV eluates (about 650-700 µl) were partially digested for 5 min at 37 °C with 25 µl of RNase-IT (Agilent) diluted to 1:50 in TNM100 buffer and the reactions were stopped using 0.4 g guanidine hydrochloride. The resulting samples were supplemented with 300 mM NaCl and 10 mM imidazole and incubated overnight at 4 °C on a stirring wheel with 50 µl Ni-NTA agarose resin slurry (QIAGEN) pre-equilibrated with wash buffer I (50 mM Tris-HCl pH 7.8, 300 mM NaCl, 10 mM imidazole, 6 M guanidine hydrochloride, 0.1% NP-40, 5 mM β-mercaptoethanol). Ni-NTA beads were then washed two times

with wash buffer I, tree times with 1 x PNK buffer (50 mM Tris-HCl pH 7.8, 10 mM MgCl2, 0.5% NP-40, 5 mM β-mercaptoethanol) and transferred into Mobicol Spin Columns.

3'miRCat-33 ligation:

The miRCat-33 3' linker was ligated to the 3' end of the RNAs on the Ni-NTA beads with 800 units of T4 RNA ligase 2 truncated K227Q (New England Biolabs) in 1 x PNK buffer / 16.67% PEG 8000 in the presence of 80 units RNasin in a total volume of 80 µl. The ligation reaction was incubated for five hours at 25 °C. Beads were washed once with wash buffer I to inactivate the RNA ligase and 3 times with 1 x PNK buffer.

5' phosphorylation:

The 5' ends of the RNAs were then radiolabeled by phosphorylation in reactions containing 1 x PNK buffer, 40 µCi of 32P-ɣ ATP and 20 units of T4 PNK (Sigma) in a total volume of 80 µl. The reactions were incubated at 37 °C for 40 min. To ensure all RNAs get phosphorylated at the 5' end for downstream ligation of the 5' linker, 1 µl of 100 mM ATP was added to the reaction mix, which was incubated for another 20 min at 37 °C. Beads were washed once with wash buffer I to inactivate the kinase and four times with 1 x PNK buffer.

5' linker ligation:

5' adaptor was ligated to the 5' end of the RNAs retained on the Ni-NTA beads. Ligation reactions contained 1 x PNK buffer, 1.25 µM of 5' adaptor, 1 mM ATP, 40 units of T4 RNA Ligase 1 (New England Biolabs) in a total volume of 80 µl. The reactions were incubated overnight at 16 °C. Beads were washed three times with wash buffer II (50 mM Tris-HCl (pH 7.8), 50 mM NaCl, 10 mM imidazole, 0.1% NP-40, 5 mM β-mercaptoethanol).

TCA precipitation of the eluate:

The material retained on the beads was then eluted using two times 200 µl wash buffer II (50 mM Tris-HCl (pH 7.8), 50 mM NaCl, 150 mM imidazole, 0.1% NP-40, 5 mM β-mercaptoethanol). Eluates were precipitated with TCA (20% final concentration) in the presence of 30 µg of glycogen (Roche) to favor precipitation. The precipitated material was resuspended in NuPAGETM LDS sample buffer (Invitrogen) with reducing agent (Invitrogen), heated 10 min at 65 °C, loaded on NuPAGETM 4-12% Bis-Tris gels (Invitrogen) and run in 1 x MOPS SDS running buffer (Invitrogen). The material was then transferred onto Amersham Protran Nitrocellulose Blotting Membrane (GE Healthcare) using a transfer buffer containing 1 x NuPAGE (Invitrogen) and 20% MeOH, for two hours at 25 V and 4 °C. The area of the membrane containing a radioactive signal at the expected size of Rpa135 protein was excised. A

membrane area at the same size was excised in the BY4741 sample lane. Membranes were soaked in 400 µl wash buffer II supplemented with 1% SDS, 5 mM EDTA and proteins were degraded using 100 µg proteinase K (Sigma) and incubation for two hours at 55 °C. RNA was extracted with phenol:chloroform:isoamyl alcohol (25:24:1), and then precipitated by addition of 1:10 volume of 3 M sodium acetate (pH 5.2), 2.5 volumes of 100% ethanol and 20 µg of glycogen. Dried RNA pellets were dissolved in ultrapure MilliQ H2O.

Reverse transcription + PCR amplification:

Synthesis of cDNAs was performed using SuperScript III reverse transcriptase (Thermo Fischer Scientific) and "RT primer" oligonucleotide (See table 1). The resulting cDNAs were PCR-amplified using LA Taq DNA polymerase (TaKaRa), a common PCR primer used for all library amplifications, (RP1) and a relevant specific index primer for multiplexing: RPI1, RPI2, RPI3, RPI4, RPI5 and RPI6.

Note that a first set of experiments was performed using L5Aa, L5Ab and L5Ac 5' linkers. "RT primer" was used for RT reactions and PCR reactions were performed using P5F and P3R oligonucleotides.

PCR product purification:

The resulting PCR products were purified by phenol:chloroform:isoamyl alcohol extraction and ethanol precipitation. After agarose gel electrophoresis (agarose "small fragments", Eurogentec) run in 1 x TBE buffer and stained with SYBR Safe DNA gel stain (Invitrogen), DNA fragments ranging in size between 150 and 250 base pairs were gel purified using MinElute PCR Purification Kit (QIAGEN). Concentration of the final DNA samples was measured using Qubit™ dsDNA HS Assay Kit (Invitrogen) and a Qubit™ fluorometer (Thermo Fischer Scientific) and the samples were sent to the Epitranscriptomics & Sequencing (EpiRNA-Seq) facility for Illumina sequencing.

Deep-sequencing and computational analyses

Sequencing was performed using an Illumina MiSeq system. Adapters and low-quality reads were eliminated using Flexbar (http://sourceforge.net/projects/flexbar/). Reads UMI barcode were extracted using umi_tools version 1.1.2. [OGT1] Reads were cleared of their adapter with cutadapt version 1.18 and cleaned reads were aligned to the yeast genome both on the entire genome version EF2.59.1 (R63-1-1) and on the rDNA sequence using Novoalign version 3.09.00 (http://www.novocraft.com). SAM files were converted (view -b), completed (fixmate), ordered (sort) using samtools version 1.14 PCR duplicates were then removed using a custom script in R, based on both start, end and umi barcode. Quality control was applied at each step using fastQC version 0.11.9 and samtools flagstat. Per base coverage based on the 3' end of the reads on the different alignments

were generated using R and in-house scripts available on our github. Downstream analyses including the pileups were performed using the pyCRAC tool suite (http://sandergranneman.bio.ed.ac.uk/Granneman_Lab/pyCRAC_software.html). Hits repartition per million of sequences were produced using pyReadCounter.py—m 1,000,000 option. Different pileups of hits for each gene were obtained using pyPileup.py—L 50—limit = 100,000 options. Raw and processed data are available in the Gene Expression Omnibus database under the accession number GSE247803. The entire pipeline, developed in Snakemake using conda environment, including our in house is available on https://github.com/CBIbigA/crac-seq/.

In vitro transcriptional assays :

Pol I purification :

RNA Pol I was purified as described in (Schwank et al., 2022) with the following modifications. Y4006, Y4007 and Y4089 strains were grown in YPD medium (2% [w/v] peptone, 2% [w/v] glucose, 1% [w/v] yeast extract) and harvested at OD_{600}~2.0. Cells were resuspended in lysis buffer (1.5mL lysis buffer per 1g cells) in cold Zirkonia tubes (6mL per 12g glass beads Ø 0.75-1mm) and mechanically lysed with Precellys Evolution (Bertin Technologies) using 6× pulse at 6000 rpm for 30s followed by 30 s pause in between. The extract was incubated with IgG sepharose beads that have been pre-equilibrated in lysis buffer on a turning wheel for 2h at 4°C (1µL bead suspension per 2mg protein). Beads were washed four times with 1mL of wash buffer (20 mM Hepes/ KOH [pH 7.8], 20% [v/v] glycerol, 5 mM MgCl2, 1500 mM KOAc, and 0.15% [v/v] NP-40) for 10min at 4°C and equilibrated three times with elution buffer (20 mM Hepes/KOH [pH 7.8], 10% [v/v] glycerol, 5 mM MgCl2, 200 mM KOAc, and 5 µM ZnCl2) for 3min at 4°C. Beads were resuspended in elution buffer (1µL elution buffer per 2µL beads suspention), incubated with TEV protease overnight at 16°C and eluate is recovered and analyzed via SDS-PAGE and Comassie staining and is used for the *in vitro* transcriptional assays.

Template generation :

The minimal transcription templates used in this study are produced as described in (Schwank et al., 2022). The oligonucleotides for template generation are listed in table 2. The RNA-DNA scaffold was diluted to 0.1 µM for subsequent RNA cleavage or elongation assays.

In vitro transcriptional assays :

RNA cleavages assay was conducted as described in (Schwank et al., 2022) with 0.2 pmol of Pol I incubated with 0.066 pmol of the respective preannealed minimal transcription cleavage scaffold in 1× transcription buffer (20 mM Hepes/KOH [pH 7.8], 10 mM MgCl2, 5 mM EGTA/KOH [pH 8.0], 5 µM ZnCl2, and 100 mM KOAc) at 4 °C for 10 to 20 min. For elongation assay, samples were implemented with NTPs (200µM final concentration of each). Samples are incubated at 28°C for 1 to 30 min. Reaction

was stopped using equal amount of 2× TBE loading dye (8 M urea, 0.08% [w/v] bromophenol blue, 4 mM EDTA/NaOH [pH 8.0], 178 mM Tris–HCl, and 178 mM boric acid. The 5'Cy5-labeled RNA was size-separated on a 20% denaturing polyacrylamide gel (20% [w/v] acrylamide/bisacrylamide [19:1], 6 M urea, 0.1% [v/v] N, N, N', N'-tetramethylethylenediamine, 0.1% [w/v] ammonium persulfate, 2 mM EDTA/ NaOH [pH 8.0], 89 mM Tris–HCl, and 89 mM boric acid) using 1× TBE running buffer (89 mM Tris–HCl, 89 mM boric acid, and 2 mM EDTA/NaOH [pH 8.0]) and visualized with a Typhoon imaging system (GE Healthcare).

RESULTS

Cells bearing SuperPol overproduce rRNA *in vivo*

We previously suggested that SuperPol is over-producing rRNA compared to WT *in vitro* (Darrière et al., 2019). This was documented using Transcription Run-On (TRO) that showed an increased transcriptional activity of SuperPol over WT enzyme. In TRO experiment, N-Lauroylsarcosine is used to permeabilize cells but also induces RNAses inhibition. Surprisingly, using northern-blot and short *in vivo* labeling experiments, we could not reveal increased pre-rRNA and/or mature rRNA accumulation *in vivo* due to SuperPol. We thus hypothesized that *in vivo* overproduced rRNAs in cells bearing SuperPol are rapidly targeted by the nuclear exosome or other cellular exonucleases. This hypothesis was supported by the detection of increased pre-rRNA production in SuperPol over WT Pol I in absence of Rrp6, the nuclear component of the exosome. rRNAs in synthesis still attached to the polymerase as well as abortive and partially degraded/processed transcripts result in a faint and smeared signal corresponding to heterogeneous RNA lengths distributed along the electrophoresis gel. Due to the short half-life of rRNAs precursor, these heterogeneous RNAs represent a significant part of Pol I transcriptional activity. In order to detect such RNAs produced by Pol I and to definitely confirm our hypothesis, we set up an experiment we called Pol I **T**ranscriptional **M**onitoring **A**ssay (Pol I TMA). This assay is initiated with a short *in vivo* pulse labeling of all newly synthesized RNAs using incorporation of Phosphorus-32 ([^{32}P]). Neosynthesized, radiolabeled RNAs are next extracted, partially fragmented and used to probe slot-blots loaded with single strand DNA fragments complementary to rDNA locus. Figure 1A shows the position of the different probes along rDNA. The use of slot-blots like in TRO, instead of gel electrophoresis to visualize radiolabeled RNAs allowed the monitoring of the heterogeneous rRNA transcripts irrespective of their synthesis/degradation status, in addition to pre-rRNAs and mature rRNAs (see figure 1). In contrast to TRO, neo-synthetized transcripts can be degraded following incorporation of radiolabeled nucleotide. To minimize the effect

of degradation in TMA readout, we determine the shortest time window required to detect labelled rRNA between [^{32}P] pulse and extraction of nascent RNA. A slight radioactive signal was already detectable after a 20 seconds labeling but we choose to pulse for 40 seconds to get a significant and reproducible signal.

Pol I TMA was performed several times using WT and cells bearing SuperPol. We used 5S rRNA signal as internal control for normalization in all further experiments. As previous analysis indicated that incorporation of [^{32}P] in the 5S rRNA transcribed by RNA polymerase III was mildly detectable (Briand et al., 2001)(data not shown, also observed using TRO (Wery et al., 2009)), we used two probes covering the entire 5S rRNA sequence to get decent signal. In parallel, IGS2 signal was used as negative control.

This novel method allowed us to confirm *in vivo* our initial TRO measurement: the observation of an increased labeled rRNA signal for Pol I transcript in Superpol, even in presence of Rrp6. Results from three independent experiments were quantified and analyses revealed a 50% increase of Pol I transcription *in vivo*, in cells bearing SuperPol compared to WT control (Figure 1B and 1C). Note that this value is probably under-estimated as degradation of some of the different transcripts still occurs during the 40s pulse. Overall, these results show that F301S mutation in Rpa135 drastically increases Pol I capability to produce rRNA. Pol I TMA is clearly an efficient method to evaluate transcriptional activity *in vivo*.

SuperPol displays a lower rate of pause compared to WT Pol I

As demonstrated previously by Miller's spread experiment and ChIP, the number of polymerases engaged in transcription in strains bearing WT Pol I and SuperPol is similar (Darrière et al., 2019). An increased rRNA production with a comparable number of Pol I engaged in transcription suggests a modification of elongation properties of SuperPol relative to WT. Thus, we compared WT Pol I and SuperPol distribution during elongation using the CRAC method developed by (Sander Granneman et al., 2009) and adapted to Pol I by (Turowski et al., 2020). This technique reveals Pol I distribution at nucleotide level along the rDNA gene. Assuming a steady state, the velocity can be interpreted from the spatial distribution. Thus, it allows to visualize the propensity of the polymerase to pause or slow-down during elongation.

The WT Pol I distribution profile we obtained is qualitatively highly similar to the one published by (Turowski et al., 2020), showing the robustness of the CRAC analysis (Figure 2A and Figure S1). When comparing WT Pol I and SuperPol global spatial distribution profiles along rDNA gene, massive accumulations are visible in 5'ETS, and to a lower extent between the 5.8S sequence and the beginning of the 25S sequence. Zooming on the 5' end of the rDNA gene, we could observe SuperPol and WT Pol I pausing at identical position, but not to the same extent (Figure 2B and Figure S1). To compare the most frequent pausing sites of Pol I and SuperPol, we computed the differences between their CRAC profiles (grey curve). This analysis revealed that SuperPol exhibits reduced accumulation at various positions between the transcription start site (TSS) and 300th nucleotide. This indicates that SuperPol likely transitions more efficiently through this region, possibly due to decreased pausing or enhanced elongation efficiency during the early stages of transcription. To highlight regions of comparatively lower pausing frequency, we also computed the ratio between distributions (excluding 27 nucleotides out the 225 nt shown here, due to low coverage). Despite a highly reproducible global profile, we could

identify local variations between Pol I CRAC nucleotide distribution replicates. Importantly, despite some local variations, we could reproducibly observe a 25% increased occupancy of WT Pol I in 5'-ETS compared to SuperPol (Figure 2C and Ffigure S1). Overall, analysis of CRAC data did not allow to identify specific sequence feature at which SuperPol and WT were differentially accumulated. However, the analysis of occupancy of SuperPol relative to WT Pol I revealed a significant decrease in the 5'-ETS.

Modified elongation properties of SuperPol impact premature termination of transcription.

This analysis of Pol I distribution using CRAC showed that increased rRNA synthesis of SuperPol is associated with modified elongation dynamics. The concept of premature termination of transcription (or PTT) as a transcriptional control of gene expression has long been established in bacteria and is referred to as "attenuation" (Artz and Broach, 1975; Bertrand et al., 1975). In yeast and mammalian cells, the study of the transcription by RNA polymerase II and III revealed PTT as a major contributor to global transcriptional regulation (Arigo et al., 2006; El Hage et al., 2008; Kamieniarz-Gdula and Proudfoot, 2019; Porrua and Libri, 2015; Steinmetz et al., 2006; Xie et al., 2023).

The occurrence of PTT during RNA Pol I transcription has only been reported following drugs poisoning Pol I elongation such as actinomycin D (Fetherston et al., 1984; Shcherbik et al., 2010). However, wild-type Pol I and SuperPol exhibit similar transcription initiation properties (Darrière et al., 2019) but different pause kinetics (Fig.2B). We hypothesized that the overproduction of rRNA in strains expressing SuperPol may stem from a reduced frequency of PTT occurrences due to shorter pauses.

Since abortive transcripts are released from transcribing Pol I, they cannot be detected by the CRAC Pol I method. Therefore, to identify abortive transcripts, we performed Northern blot analysis. Premature transcription termination (PTT) is known to produce abortive transcripts that are generally unprocessed. Once released from Pol I, their 3' ends become accessible to cellular exonucleases. As a result, these RNAs have a very short half-life and only accumulate when 3'-5' exonucleases, such as

the RNA exosome, are inhibited. ((Kamieniarz-Gdula and Proudfoot, 2019) and see figure 3A). We therefore undertook a search for abortive rRNAs in order to compare their accumulation in strains expressing wild-type Pol I or SuperPol. According to our hypothesis, such transcripts would be produced in higher amount in WT strains compared to mutant bearing SuperPol. To reveal abortive transcripts, we performed Northern blot analysis in presence and absence of Rrp6, the nuclear specific 3'-5' exonuclease subunit of the RNA exosome (Fig. 3B). Therefore, Rrp6-sensitive accumulation of rRNA indicate transcripts with an accessible 3'-end.

This experiment reveals the existence of such transcripts at the proximity of TSS. The size of one of them is comprised between 70 and 90 nts and is accumulated in absence of Rrp6 (Figure 3B, lane 3). Interestingly, the accumulation of these abortive transcripts is greatly reduced in SuperPol background (Figure 3B, lane 4, quantified in Figure 3C). Note that , other known rRNA species resulting from degradation products of full ETS1 by the exosome are accumulated in this area (≈130 and 160nt long) (Delan-Forino et al., 2017). As opposed to abortive transcript, those degradation products are detected in both WT and SuperPol.

These results unveil a massive amount of abortive rRNAs produced by Pol I. To investigate if the altered PTT rate in SuperPol accounts for its 1.5 fold increased full length rRNA synthesis relative to WT Pol I, a Cumulative Distribution Function (CDF) analysis of Pol I CRAC profiles across the 6861 nucleotides of the entire 35S rRNA (Figure 3D). The CDF of SuperPol shifts rightward, indicating reduced accumulation in the 5' region of the gene relative to WT Pol I. Altogether, we propose that SuperPol is more processive than WT Pol I as this low pausing rate is associated with a reduction in the quantity of abortive transcription events.

The enzymatic properties of SuperPol result in reduced cleavage activity and increased elongation dynamics, to the detriment of transcriptional fidelity.

Pol I elongation is a discontinuous and stochastic process based on Brownian ratchet motion, making it prone to frequent pausing, backtracking and RNA cleavage to restart elongation.

In order to characterize SuperPol enzymatic properties, we first performed *in vitro* cleavage assays (Merkl et al., 2020; Pilsl et al., 2016a, 2016b; Schwank et al., 2022). WT Pol I and SuperPol have been purified several times from yeast cells expressing a HTP-tagged subunit Rpa135 (Figure 4A and Figure 4B and Figure S2). RNA cleavage was monitored using an RNA/DNA hybrid scaffold containing 3 nucleotides mismatch at the RNA 3′end (clv3) (Figure 5A). The scaffold was then incubated with purified Pol I elongation complex in absence of ribonucleotides from 1 to 30 minutes. Results shown in Figure 5B (quantified in Figure 5C) show that WT Pol I cleaves off 2 nt of the RNA fragment used as substrate after 5 minutes. A second cleavage of 4 nt become predominant after 30 minutes. However, SuperPol cleaves mainly at the position -2 and only few -4 RNA fragment are detected compared to WT Pol I, even after 30 minutes. This assay shows that SuperPol cleavage activity is affected in these conditions, leading to decreased ability to remove mismatched nucleotides compared to WT Pol I.

We next tested if following cleavage, SuperPol transcriptional activity was increased using *in vitro* elongation assays (Merkl et al., 2020; Pilsl et al., 2016a, 2016b; Schwank et al., 2023)(Merkl et al., 2020; Pilsl et al., 2016a, 2016b; Schwank et al., 2022). RNA elongation was monitored using an RNA/DNA hybrid scaffold containing 1 nucleotide mismatch at the RNA 3′end (clv1) (Figure 5D). The scaffold is then incubated with purified Pol I elongation complex in absence or presence of ribonucleotides from 1 to 30 minutes. The RNA, which contains a Cy5 fluorophore at its 5′end, is detected on a denaturing polyacrylamide gel.

The results show that in absence of nucleotides, both WT Pol I and SuperPol cleave off 1 or 2 nt of the RNA fragment used as substrate after 30 minutes, thus removing the 3’ nucleotide mismatch (Figure 5E). We used this specific mismatch template because we noticed that -1 and -2 RNA fragments are detected in the same amount both with WT Pol I and SuperPol (compare Figure 5E: lane 2 and 7). When polymerases are incubated in presence of ribonucleotides, the RNA fragment cleaved at -2 can

now be used as substrate to elongate up to the end of the DNA template, resulting in the production of a +14nt-long RNA. From 1 minute to 30 minutes of incubation with ribonucleotides, the production of this +14nt RNA is 2-fold higher by the SuperPol compared to WT Pol I (Figure 5E, quantified in Figure 5F). This result shows that SuperPol displays an improved ability to resume elongation following cleavage compared to WT Pol I. This assay has been reproduced several times with the use of 4 independent polymerase purifications (see supplementary Figure 2).

Finally, we compared the error rates for WT Pol I and SuperPol during elongation. To investigate this feature *in vitro*, a DNA-RNA template including no mismatches (ext1; Figure 5G) is incubated with GTP and ATP. The GTP, which is complementary to the +1 position of the DNA template at the 3' end of the hybridized RNA, should be correctly incorporated by the elongation complex in order to produce a +1nt RNA product. The detection of a +2nt RNA indicates a misincorporation event. An increased +2nt product reveals that SuperPol is more prone to misincorporate nucleotides compared to WT Pol I (Fig 5H). A strain lacking the C-terminal part of the subunit Rpa12, which is required for cleavage activity, was used as a control. This strain cannot cleave misincorporated nucleotides and thus display the highest rates of misincorporation. Quantification of this assay (Figure 5I) allowed us to determine that SuperPol misincorporation rates are intermediate between those of WT Pol I and the WT bearing the Rpa12ΔC truncation.

Based on these *in vitro* transcriptional assays, we concluded that SuperPol exhibits enhanced elongation dynamics compared to wild-type Pol I. Specifically, the elongation assays showed that SuperPol elongates the RNA substrate at a rate approximately two-fold higher than that of the wild-type enzyme when ribonucleotides are present. This increased elongation is sustained over time, as evidenced by the more rapid production of the +14nt RNA fragment, reinforcing the notion that

SuperPol has improved processivity both *in vivo* and *in vitro*, albeit at the expense of a higher nucleotide misincorporation than the WT enzyme.

SuperPol is resistant to BMH-21 and retains high levels of transcription upon BMH-21 treatment

BMH-21 is a small-molecule that was previously identified in a high-throughput screen for anticancer agents in Laiho's laboratory (Peltonen et al., 2010). It has been reported that BMH-21 is a DNA intercalator that preferentially and non-covalently binds to regions rich in GC islands, without activating the DNA damage response (Colis et al., 2014; Peltonen et al., 2010). In mammalian cells, BMH-21 rapidly and efficiently blocks Pol I-mediated transcription, and induces proteasome-dependent degradation of the largest Pol I subunit, RPA194 (Peltonen et al., 2014b). This effect is characteristic of BMH-21 and is conserved in the yeast *Saccharomyces cerevisiae*. Treatment of a yeast strain with BMH-21 specifically affects Pol I transcription elongation, induces the degradation of Rpa190 and strongly reduces cell viability (Wei et al., 2018). Indeed, Pol I transcription elongation complexes appear to be a preferential substrate for Pol I subunit degradation when cells are exposed to BMH-21.

To challenge our model suggesting that SuperPol has modified elongation capabilities, we exposed mutant cells expressing SuperPol, as well as wild-type (WT) controls, to BMH-21 and measured cell viability, rRNA synthesis, and Pol I subunits abundance.

Cell viability was assessed using serial dilutions to evaluate number and size of individual colonies (Figure 6A). Growth of WT and mutant cells was indistinguishable in media without BMH-21. In the presence of a low concentration of BMH-21 (17µM), the growth of WT cells showed a slight growth delay compared to condition in which no BMH-21 was added. In contrast, the growth of cells bearing SuperPol was insensitive to such BMH-21 concentration. The contrast was even more pronounced when 35µM of BMH21 was added to the growth media. While the growth of cells expressing SuperPol is only slightly affected, the fitness of WT cells was severely reduced under the

same conditions. These results show that cells expressing SuperPol are resistant to BMH-21. Note that both WT and SuperPol were unable to support growth when BMH-21 was added in the media at a concentration of 50µM.

We next performed Pol I TMA experiments to evaluate if *RPA135-F301S* mutation affects RNA Pol I activity in response to BMH-21. WT and SuperPol strains were incubated with 35µM or 50µM BMH-21 or DMSO for 30 minutes before Pol I TMA was initiated. Compared to Pol III, the Pol I activity of WT strains specifically dropped to 70% when incubated with 35µM BMH-21 and to less than 30% in case of treatment with 50µM BMH-21 (Figure 6B). In contrast, SuperPol retained almost 80% of its activity, even after a 30 minutes incubation with 50µM BMH-21.

BMH-21 exposure results in proteasome-dependent degradation of the RNA Pol I largest subunit RPA194/Rpa190 in both human and yeast cells (Peltonen et al., 2014b; Wei et al., 2018). We thus assessed Pol I subunits accumulation in presence of BMH-21 in *RPA135-F301S* cells and compared it to WT. The cells were treated with 35µM of BMH-21 and aliquots were collected at 15 minutes, 30 minutes and 2 hours. Pol I subunits accumulation was evaluated using anti-Pol I antibody raised against the entire enzyme (Figure 6C). As previously observed (Wei et al., 2018), Rpa190 in WT cells is rapidly destabilized by proteasome-dependent degradation after 15min of treatment with BMH-21, to reach less than 20% of its original level after 2 hours (Figure 6D, left panel). More surprisingly, we also observed a similar decrease in the accumulation of Rpa135 in the same condition, which led to an 80% degradation of the protein (Figure 6D, right panel). In contrast, the other Pol I subunits did not show such reduced accumulation. Rpa190 and Rpa135 exhibited a different behavior in cells expressing SuperPol. Although the exposure to high concentrations of BMH-21 affected the levels of these two subunits, 70% of their initial level remains. We concluded that the RPA135-F301S mutation decreased the proteasome-dependent degradation of the two largest subunits of Pol I in presence of BMH-21, allowing a robust ribosomal RNA production in presence of the drug.

BMH-21 reduces Pol I occupancy through targeting of paused Pol I and stimulation of premature termination

To better understand the impact of BMH-21 on the elongation properties of WT Pol I and SuperPol, we analyzed by CRAC the enzyme distribution along rDNA and the production of abortive transcripts in presence or absence of BMH-21, (Figure 7). Importantly, we used a short exposure to BMH-21 to ensure that Pol I was not massively depleted *in vivo*. Using Net-seq, Schneider's lab reported that BMH-21 treatment leads to a decrease in WT Pol I occupancy *in vivo* in rDNA spacer regions, 5' external transcribed spacer (5'ETS), internal transcribed spacer 1 (ITS1), internal transcribed spacer 2 (ITS2), 3'external transcribed spacer 2 (3'ETS) (Jacobs et al., 2022). CRAC results confirmed that WT Pol I occupancy has strongly decreased in these regions (Figure 7A). The difference between frequency of reads shows that the loss of WT Pol I accumulation in presence of BMH-21 is spread along the 5'ETS and not located at specific positions as observed with SuperPol (see Figure 2). The ratio between distributions reaches 2-fold less accumulation in presence of BMH-21, notably around the 100th nucleotide and between the 200th and the 230th nucleotide (Figure 7A).

CRAC data show that BMH-21 effects on Pol I elongation are specifically localized in regions where WT Pol I is highly accumulated, notably in the 5'ETS. This result suggests that BMH-21 specifically targets paused elongation complexes. Comparison of WT Pol I and SuperPol occupancy in presence of BMH-21 show that SuperPol occupancy is less affected by the drug (Figure 7B). We could show that SuperPol exhibits a decreased pausing relative to WT enzyme, which is consistent with the fact that SuperPol retains high levels of transcription upon BMH-21 treatment (see figure 6).

In vitro transcription reaction experiments published by (Jacobs et al., 2022) shows that BMH-21 treatment increases pausing of the elongation complex, and globally reduces the amount of Pol I elongation complexes capable of processive transcription. However, *in vivo*, both NET-seq and CRAC show a decreased occupancy on 5'end of rDNA, compatible with a putative massive premature termination *in vivo*.

We next measured the production of abortive rRNA in vivo, as presented earlier, by a northern blot using TSS probes with or without Rrp6 (Figure 7C and D). Cells were treated with 35 µM BMH-21 for 30 minutes. For the strain bearing WT Pol I, a very strong accumulation of short rRNA species between 70 and ≈ 300 nucleotides long is detected (black arrows). The production of abortive transcripts is massively stimulated by BMH-21. Strains bearing SuperPol are less affected by the drug treatment and the production of these abortive rRNA is mildly increased. This result suggests that BMH-21 stimulates premature termination of the WT Pol I.

Overall, these data suggest that the BMH-21 targets Pol I paused elongation complexes and stimulates their premature terminations with production of abortive transcripts. As SuperPol results in a modified pausing pattern, less prone to premature termination, this mutant form is less affected by the drug and is resistant to its inhibitory effect on rRNA transcription elongation.

Discussion

In our study, we characterized a mutant of Pol I, SuperPol, to better understand, by contrast, how rRNA production is regulated *in vivo*. We demonstrated that SuperPol overproduces rRNAs by reducing the rate of premature termination of transcription *in vivo*. The enzymatic properties of SuperPol indeed result in reduced cleavage activity, improved processivity *in vitro*, but reduced fidelity. Finally, SuperPol is resistant to BMH-21 and retains high levels of transcription upon BMH-21 treatment. Therefore, we propose that BMH-21 acts on Pol I through targeting paused Pol I and stimulating premature termination. Overall, we propose that premature termination of transcription by Pol I can be modulated. It can either be alleviated in the mutant, allowing increased rRNA production, or specifically enhanced by a drug, resulting in rapid inhibition of rRNA synthesis.

Pol I is prone to PTT and PTT is stimulated by BMH-21

PTT was first described in bacteria in the mid-1970s and was referred as "attenuation". In mammals, Pol II PTT is now considered as a major and widespread regulatory mechanism of the protein-coding genes at the transcriptional level. In this study, we have identified for the first time, PTT during Pol I transcription in WT cells under normal growth conditions. We propose that stalled Pol I is inherently prone to premature termination. The occurrence of PTT during RNA Pol I transcription has previously been reported only following DNA-binding drugs poisoning Pol I elongation (Fetherston et al., 1984; Hadjiolova et al., 1995; Shcherbik et al., 2010).

In our study, we propose that BMH-21, known to inhibit elongation, strongly stimulates premature termination. Experiments conducted in Schneider's lab *in vitro* have shown that BMH-21 causes a delay in Pol I promoter escape efficiency, reduces Pol I elongation rate and increases Pol I pausing (Jacobs et al., 2022). Using NET-seq, the authors observed a significant decrease in Pol I occupancy in the 5'ETS region, an observation fully compatible with our model. BMH-21 has been

shown to lead to proteasome-dependent degradation of actively transcribing Pol I (Wei et al., 2018). In our study, we were able to substantiate these findings by demonstrating that BMH-21 treatment results in the degradation of Rpa190. Furthermore, we extended the initial discovery by revealing that both the largest subunit, Rpa190, and Rpa135 are destabilized by proteasome-dependent degradation, with no apparent effects on the other subunits. However, the precise mechanism behind the degradation of Rpa190 and Rpa135 remains to be clarified.

Recently, another Pol I allele resistant to BMH-21 was identified (Ibars et al., 2023). The Torres-Rosell's lab demonstrated that Nse1, an ubiquitin ligase subunit of the Smc5/6 complex, promote ubiquitination of Rpa190 at position K408 and K410. A double substitution of lysines at position 408 and 410 with arginines, named Rpa190-KR, prevents ubiquitination of Rpa190, and confers resistance to BMH-21 (Ibars et al., 2023). Upon BMH-21 treatment, Rpa190-KR, similarly to SuperPol, shows resistance to proteasome-mediated degradation of both Rpa190 and Rpa135. Furthermore, SuperPol and Rpa190-KR have a synergistic effect on BMH-21 resistance (unpublished data), suggesting a potentially distinct mechanism. We now need to untangle the relationship between PTT stimulation, ubiquitination of Rpa190 and degradation to gain a better understanding of the specificity of BMH-21.

Is transcriptional pausing coupled to premature termination of transcription?

Pol II PTT is frequent, can occur near the transcription start site (TSS) or within the gene body, and opposes the formation of full-length and functional transcripts, thereby negatively regulating gene expression. The release of the premature transcript from the elongating complex is thought to be preceded by a pause of the polymerase. The study of mammalian transcription by RNA polymerase II suggested a concordant relationship between pause time and PTT: the longer is the pause, the more frequent is the release of Pol II from chromatin at the vicinity of the promoter (Krebs et al., 2017; Steurer et al., 2018). The timing of RNA Pol II pauses during transcription elongation plays a pivotal role in the regulation of gene expression. Extended pause durations can disrupt the transcription

process, potentially resulting in incomplete mRNA formation or incorrect splicing events (for a review, see (Noe Gonzalez et al., 2021)). Pol II's residence time downstream of the transcription start site was investigated at a single-molecule level in Drosophila. Similar high Pol II turnover rates were observed downstream of promoters for both "paused genes" and "normally elongating genes" (Krebs et al., 2017). This observation demonstrates that Pol II, when stalled downstream of the promoter, is rapidly subjected to PTT with fast reinitiation cycles, rather than stable pausing. This interpretation is further supported by a study using fluorescence recovery after photobleaching (FRAP) in live human cells (Steurer et al., 2018). Computational modeling suggested that up to 90% of paused Pol II downstream of the promoter leads to PTT, with only 8% yielding a full-length mRNA. Therefore, the continuous release and reinitiation of Pol II in the vicinity of the promoter are an important component of transcriptional regulation. These results strongly suggest a coupling between pause time and PTT: the longer the pause, the larger the fraction of Pol II released from chromatin.

Concerning Pol I, this aspect of regulation was not addressed so far. We propose that stalled RNA Pol I can be subjected to PTT rather than stable pausing. CRAC Analysis ((Turowski et al., 2020) and this study) as well as EM studies of Miller chromatin spreads demonstrated uneven distribution of polymerases along the rDNA gene, indicating different elongation rates due to differing pause durations. We propose that, at a given position, the duration of the pause could regulate the fate of the Pol I elongation complex. A Pol I mutant with an increased pausing frequency and a reduced transcriptional elongation rate (Viktorovskaya et al., 2013) has been associated with rRNA processing defects resulting in an impaired ribosome biogenesis (Huffines et al., 2022). This phenotype may be the consequence of an increased rate of PTT.

Conversely, the SuperPol mutant, which exhibits a lower pausing rate, shows reduced levels of PTT. As a result, this mutant is capable of producing 1.5 times more rRNAs than the wild type. It is worth noting that no processing defect (Darrière et al., 2019) nor co-transcriptional modification defect (ribomethSeq, data not shown) was observed in SuperPol mutant when the integrity of the exosome is maintained. This suggests that putative aberrant pre-rRNAs produced consecutively to

shorter pauses do not accumulate as long as the quality control mechanisms are efficient. In summary, overall fine-tuning pausing time may be necessary to strike a compromise between slow but inefficiently productive elongation and fast but error-prone elongation, respectively.

What could be the biological relevance of Pol I pausing associated with PTT ?

The average Pol I elongation rate is significantly reduced throughout the 5' external transcribed spacer (ETS) region, where both massive early pre-rRNA assembly events and frequent PTT occur. The amount of protein bound to the 5' ETS corresponds to 40% of the total mass of the 90S preribosomal particle (Sun et al., 2017). Furthermore, studies in yeast have demonstrated that the 5' region of rRNA can pull down and crosslink the UTP-A complex (Hunziker et al., 2016; Zhang et al., 2016). The recruitment of the UTP-A complex is of paramount importance as it is a prerequisite for the assembly of all other small-subunit processome subcomplexes. We propose that Pol I pausing in the first 300 nucleotides downstream of the transcription start site (TSS) offers a window of opportunity for quality control: the UTP-A assembly onto the nascent transcript. Utp9, Utp8, and Utp17 are the UTP-A components that are recruited the closest to the 5' end, within the first 60 nucleotides of the 5' ETS. We speculate that the resumption of Pol I elongation from this point depends on the assembly of these three proteins. In absence of UTP-A binding, extended pausing would stimulate PTT and the production of a ≈80nt long abortive transcript. Similarly, Utp4, Utp5, Utp10 and Utp15 associate later to 5' ETS, up to position +350 and we also detect abortive transcripts in this range, suggesting similar quality control points in this area. This speculative model is supported by the fact that UTP-A components, notably Utp5, Utp15 and Utp17, are required for optimal rDNA transcription, as observed in Run-on analyses (Gallagher et al., 2004)

Conclusion:

In conclusion, the control of pause durations in RNA Pol II and RNA Pol I transcription elongation is of utmost importance for precise gene expression regulation. Excessive prolongation of pause durations can lead to transcriptional deregulation, while the strict regulation of pause durations ensures accurate transcription. Understanding the dynamics of pause durations in transcriptional processes is crucial for unraveling the intricacies of gene expression.

Limitations of the study

In experiments presented here, we likely underestimating the occurrence of PTT for Pol I. Our study established premature termination of transcription by focusing on production of abortive transcript only detected in absence of Rrp6. The novel implication of torpedo-like mechanism of premature release in 5'ETS and 3'ETS, as proposed by Turowski and Tollervey (Petfalski et al., 2025) strongly suggest that PTT is also occurring following Rat1 dependent degradation of nascent rRNA. Taken together, premature transcription termination (PTT) associated with transcript release, or coupled with the torpedo mechanism, is likely to represent a prominent regulatory step in the transcription cycle of rDNA.

ACKNOWLEDGMENTS

We are very grateful to our team members for critical reading of the manuscript and Vincent Rocher for bioinformatic analysis. We thank the “Ligue Nationale Contre le Cancer” for supporting CA. We acknowledge the members of the Gadal's lab for help, advice and discussion. We are very grateful to Virginie Marchand and Iouri Motorine for the EpiRNA-Seq facility in Nancy for the help and sequencing CRAC experiments. This work also benefited from the assistance of the Big-A facility of the CBI for the process and the analysis of CRAC data.

FUNDING

This work was supported by the “Fondation ARC pour la Recherche sur le Cancer” (ARCPJA 20191209547 and ARCPJA22020060002067) and the “Ligue Nationale Contre le Cancer” (3FI14194UPAL). CA was funded by a Ph.D. fellowship from the “Ligue Nationale Contre le Cancer” (TAGF23235).

CONFLICT OF INTEREST

The authors declare that they have no conflict of interest.

LEGENDS

Figure 1: Cells bearing SuperPol overproduce rRNA in vivo

Figure 1A: Yeast rDNA unit is represented, with the position of the corresponding antisense oligonucleotides used to load Slot blots (see Materials and methods for description).

Figure 1B: Pol I TMA was performed in RPA135:F301S and otherwise isogenic wild-type cells grown to mid-log phase in Phosphate depleted YPD medium. Nascent transcripts were labelled with Phosphorus-32 ([32P]) for 40 seconds. 3' marked newly synthesized RNAs were extracted, partially hydrolyzed and revealed using slot-blots. Each labeling was performed independently in triplicate; one representative example is shown in the panel.

Figure 1C: Results represented in panel B were quantitated.

IGS2 and Pol I (5'ETS, 18S.2, 25S.1 and 3' ETS) are quantified relative to 5S signal in the lower panel. Error bars indicate mean +/- SD. *** P < 0,005 ; ** P < 0 . 01 ;* P < 0 . 05 , calculated by two-sample t -test.

Figure 2: SuperPol displays a lower rate of pause compared to WT Pol I

Figure 2A: CRAC distribution profiles obtained for WT Pol I (Blue line) and SuperPol (Red line). Lines correspond to the mean frequency of reads obtained for three independent experiments. The area of the 35S rDNA gene has been highlighted (5'ETS from +1 to 700nt ; 18S from 701 to 2499nt ; ITS1 from 2500 to 2858nt ; 5.8S from 2859 to 3019nt; ITS2 from 3020 to 3250nt; 25S from 3251 to 6647nt; 3'ETS from 6648 to 6859nt).

Figure 2B: Zoom in 5'ETS CRAC distribution profiles obtained for WT Pol I (Blue) and SuperPol (Red). Lines correspond to the mean frequency of reads obtained for three independent experiments while the colored area corresponds to the min-max range of the three experiments. The grey area corresponds to the difference between WT Pol I and SuperPol frequency of reads at each position of the gene. This difference has been calculated using the min-max range values giving the lowest difference (white area between blue and red min-max range). The lower panel represents the ratio

between WT Pol I and SuperPol, represented in log2. Blue areas correspond to sequences where WT is more accumulated than SuperPol and red areas correspond to the sequences where SuperPol is more accumulated than WT Pol I.

Figure 2C: Frequency of reads obtained for each 35S area (5'ETS, 18S, ITS1, 5,8S, ITS2, 25S, 3'ETS) from three independent experiments were summed and shown as mean+/- SD. *** P < 0,005 ; ** P < 0 . 01 ;* P < 0 . 05 , calculated by two-sample t -test.

Figure 3: Modified elongation properties of SuperPol impact premature termination of transcription.

Figure 3A: Events of premature terminations lead to the releasing of both stalled Pol I elongation complex and nascent transcript. The 3'end of these abortive transcripts is not protected anymore by the elongation complex and become accessible to degradation by rrp6, the 3' to 5' exonuclease nuclear subunit of the exosome. To accumulate and detect abortive transcripts, deletion of rrp6 is necessary.

Figure 3B: Cells bearing WT Pol I or SuperPol, with or without rrp6, were grown and total RNAs were extracted and analyzed by northernblot using TSS probes. Low molecular weight RNA products were resolved on 8% Polyacrylamide/8.3M urea gels.

Figure 3C: Low molecular weight RNA (≈ 80nt) products were quantified relative to 5S signal. Error bars indicate mean +/- SD. *** P < 0,005 ; ** P < 0 . 01 ;* P < 0 . 05 , calculated by two-sample t -test.

Figure 3D: Cumulative Distribution Function (CDF) of Pol I profiles obtained by CRAC on the 6861 nucleotides of the rDNA. The cumulative distribution of both WT Pol I and SuperPol are represented respectively by the blue and red curves. Lines correspond to the mean cumulative distribution of frequency of reads obtained for three independent experiments while the colored area corresponds to the min-max range of the three experiments.

Figure 4: Purification of RNA Pol I and SuperPol

Figure 4A: Tagged WT Pol I and SuperPol were immunopurified respectively from yeast strains #3207 and #3208. Purified fractions were migrated and separated on 4-12% SDS-PAGE and revealed by Coomassie Blue (see Materials and Methods).

Figure 4B: Tagged WT Pol I and SuperPol were immunopurified respectively from yeast strains #3207 and #3208. Purified fractions were analyzed by western blot using anti-Pol I antibody (see Materials and Methods).

Figure 5: Enzymatic properties of SuperPol result in altered cleavage activity and increased elongation activity

Figure 5A: DNA–RNA hybrid scaffold with three mismatched nucleotides at the RNA 3'end used for cleavage assays (clv3). The RNA contains a fluorescent Cy5 label on the 5'RNA end. Cleavage sites are indicated relatively to the 3'end of the RNA (site 0).

Figure 5B: About 0.15 pmol of either WT Pol I or SuperPol were added to 0.05 pmol cleavage scaffold and incubated for the indicated time intervals. Fluorescent transcripts were analyzed on a 20% denaturing polyacrylamide. RNAs shortened by two (-2) or four (-4) nucleotides and uncleaved RNAs (0) are indicated.

Figure 5C: Quantification of cleavage efficiency (uncleaved (0) RNA) and the accumulation of -2 and -4 RNA from three independent assays. Values are indicated as percentage of (0) uncleaved RNA after incubation of scaffold template clv3 with WT Pol I and SuperPol.

Figure 5D: DNA–RNA hybrid scaffold with one mismatched nucleotide at the RNA 3'end used for elongation assays (clv1). The RNA contains a fluorescent Cy5 label on the 5'RNA end. Cleavage sites are indicated relatively to the 3'end of the RNA (site 0).

Figure 5E: About 0.15 pmol of either WT Pol I or SuperPol were added to 0.05 pmol cleavage scaffold and incubated with or without nucleotides (200 µM final concentration of each) for the indicated time intervals. Fluorescent transcripts were analyzed on a 20% denaturing polyacrylamide gel. Uncleaved

RNAs (0), RNAs shortened by two (-2) nucleotides and elongated RNAs (from +1 to +14) and are indicated with corresponding sequence.

Figure 5F: Quantification of elongation efficiency (+14nt RNA elongation product) from three independent assays. Values were quantified relative to (0) uncleaved RNA after incubation of scaffold template clv1 with WT Pol I and SuperPol, with or without nucleotides. Error bars indicate mean +/- SD. *** P < 0,005 ; ** P < 0 . 01 ;* P < 0 . 05 , calculated by two-sample t -test.

Figure 5G: RNA–DNA hybrid scaffold including no mismatches used for misincorporation assays (ext1). The RNA contains a fluorescent Cy5 label on the 5'RNA end. Ribonucleotides to be incorporated are indicated in grey.

Figure 5H: About 0.2 pmol Pol I WT, 0.2 pmol SuperPol and 0.2 pmol Pol I Rpa12ΔC were incubated with 0.066 pmol RNA–DNA scaffold for 20 min on ice. Mixtures of GTP and ATP (200 µmol) were added, and samples were incubated at 28°C for the indicated time intervals. Resulting transcripts were analyzed on a 20% denaturing polyacrylamide gel. RNAs shortened by one (-1) nucleotides, uncleaved RNAs (0) and extended RNAs by one (+1) and two (+2) nucleotides are indicated. Note that production of +2 RNAs reveals misincorporation as the second nucleotide to be incorporated should be UTP and not GTP nor ATP.

Figure 5I: Quantification of misincorporation from three independent assays. The production of elongated RNA resulting from misincorporation (+2) relative to uncleaved RNA (0) from WT, SuperPol and Rpa12ΔC was quantified. Note that significant misincorporation of SuperPol relative to WT is detected after a 20-minute incubation. Error bars indicate mean +/- SD. *** P < 0,005 ; ** P < 0 . 01 ;* P < 0 . 05 , calculated by two-sample t -test.

Figure 6: SuperPol is resistant to BMH-21 and retains high levels of transcription upon BMH21 treatment.

Figure 6A: SuperPol suppresses the growth defect due to BMH-21 in the yeast *S. cerevisiae*. Ten-fold serial dilutions WT and RPA135-F301S single mutant were spotted on rich media to assess growth at 30°C in presence of various concentration of BMH-21 or vehicle. Growth was evaluated after two days.

Figure 6B: Cells bearing SuperPol keep strong Pol I transcriptional activity upon BMH21 treatment. Pol I TMA allowing detection of accumulated newly synthesized RNA during the pulse. Nascent transcripts were labelled, and revealed using antisens oligonucleotides immobilized on slot-blot as described in Figure 1 and Materials and Methods. IGS2, Pol I (mean of 5'ETS, 18S.2, 25S.1, 3' ETS) are quantified relative to 5S signal in the right panel. Yeast rDNA unit is represented in the upper panel, with the position of the corresponding antisense oligonucleotides used.

Figure 6C: Cells bearing SuperPol maintained high levels of Rpa190 and Rpa135 upon BMH-21 treatment. WT and RPA135-F301S cells were incubated with 35µM of BMH21 or DMSO. Aliquots were collected at 15 minutes, 30 minutes and 2 hours and Pol I subunits accumulation was assessed using anti-Pol I antibody (see Materials and Methods).

Figure 6D: Accumulation of the two largest Pol I subuntis Rpa190 (left panel) and Rpa135 (right panel) upon BMH-21 treatment is quantified relative to control condition (DMSO). Error bars indicate mean +/- SD. *** P < 0,005 ; ** P < 0 . 01 ;* P < 0 . 05 , calculated by two-sample t -test.

Figure 7: BMH-21 reduces Pol I occupancy through targeting of paused Pol I and stimulation of premature termination

Figure 7A: Zoom in 5'ETS CRAC distribution profiles obtained for WT Pol I (Blue) and WT Pol I incubated with 35µM of BMH-21 for 30 minutes (Green). In the upper panel, lines correspond to the mean frequency of reads obtained for two independent experiments while the colored area corresponds to the min-max range of the two experiments. The grey area corresponds to the difference of frequency of reads at each position of the gene between WT Pol I and WT Pol I with BMH-21. This difference has been calculated using the min-max range values giving the lowest difference (white area between blue and red min-max range). The lower panel represents the ratio between WT Pol I and WT Pol I with BMH-21, represented in log2. Blue areas correspond to sequences where WT Pol I without BMH-21 is

more accumulated and green areas correspond to the sequences where WT Pol I incubated with BMH-21 is more accumulated.

Figure 7B: Zoom in 5'ETS CRAC distribution profiles obtained for SuperPol (Red) and SuperPol incubated with 35µM of BMH-21 for 30 minutes (Yellow).

Figure 7C: Cells bearing WT Pol I or SuperPol, in presence or in absence of Rrp6, were grown and treated with 35µM of BMH-21 for 30 min. Total RNAs were extracted and analyzed by northern blot using TSS probe. Abortive transcripts are indicated by arrows.

Figure 7D: Premature transcript products were quantified relative to 5S signal (focusing on ≈80 nt size). Error bars indicate mean +/- SD. *** P < 0,005 ; ** P < 0 . 01 ;* P < 0 . 05 , calculated by two-sample t -test.

Strains used in this study :

Strain	Name	Genotype	Plasmid	Origin or reference
0480	BY4741	*MAT a, his3Δ1, leu2Δ0, lys2Δ0 ura3Δ0*		This study
2742	OGT32-1a	*MAT a, his3Δ1, leu2Δ0, lys2Δ0 ura3Δ0, RPA135-F301S::URA3*		This study
2743	yCD2-1a	*MAT a, his3Δ1, leu2Δ0, lys2Δ0 ura3Δ0, rrp6::NAT*		This study
2744	OGT33-1a	*MAT a, his3Δ1, leu2Δ0, lys2Δ0 ura3Δ0, RPA135-F301S::URA3,* rrp6::NAT		This study
3207	yCA3-1a	*MAT a, his3Δ1, leu2Δ0, lys2Δ0 ura3Δ0, RPA135-HTP::URA3*		This study
3208	yCA2-1a	*MAT a, his3Δ1, leu2Δ0, lys2Δ0 ura3Δ0, RPA135-F301S-HTP::URA3*		This study
	Y4006	MATa his3Δ1 leu2Δ0 lysΔ0 ura3Δ0 RPA135-F301S::URA3 KANMX-pGAL::RPA12	pCM182-LEU2-RPA12	(Schwank et al., 2022)
	Y4007	MATa his3Δ1 leu2Δ0 lysΔ0 ura3Δ0 RPA135-F301S::URA3 KANMX-pGAL::RPA12	pCM182-LEU2-rpa12delC (aa 1-69)	(Schwank et al., 2022)

Oligonucléotides used in this study:

Name	5’-3’ Sequence
774	GTCTTCAACTGCTTTCGCAT
1855	AAATGGCCTATCGGAATACATTTTCTACATCCTAACTACTATAAAACAACCTTTAGACTTACGTTTGCTACTCTCATGGT
1856	TACAAAAACATAACGAACGACAAGCCTACTCGAATTCGTTTCCAAACTCTTTTCGAACTTGTCTTCAACTGCTTTCGCAT
1857	TGCGACCGGCTATTCAACAAGGCATTCCCCCAAGTTTGAATTCTTTGAAATAGATTGCTATTAGCTAGTAATCCACCAAA
1858	TATCTTAAAAGAAGAAGCAACAAGCAGTAAAAAAGAAAGAAACCGAAATCTCTTTTTTTTTTTCCCACCTATTCCCTCTT
1859	GGAATTCCTCGTTGAAGAGCAATAATTACAATGCTCTATCCCCAGCACGACGGAGTTTCACAAGATTACCAAGACCTCTC
1860	GTGCTGGCCTCTTCCAGCCATAAGACCCCATCTCCGGATAAACCAATTCCGGGGTGATAAGCTGTTAAGAAGAAAAGATA
1861	GTAAATGGTACACTCTTACACACTATCATCCTCATCGTATATTATAATAGATATATACAATACATGTTTTTACCCGGATC
1863	CAGCTTAACTACAGTTGATCGGACGGGAAACGGTGCTTTCTGGTAGATATGGCCGCAACCGATAGTTTAACGGAAACGCA
1864	AAAAAAAAAAAAGAAATAAAGATTGCAGCACCTGAGTTTCGCGTATGGTCACCCACTACACTACTCGGTCAGGCTCTTAC
1898	CCTCTATATGATACAATTGACCAAGCCTTCATTTACCATTCTATATCAATTTGGAAAGAAGGGTATTTCTTACGACTCACTATAGGG
1899	TGAAGTACTTGGACTCTGAGCTATCCGGCAATGGGTATAAGATTGCGTTATAATGTAGAGCCCAAAGAGCACCATCACCATCACCATGATTATGATATTCC
miRCat-33 3’	rAppTGGAATTCTCGGGTGCCAAG/ddC/
5’ adaptor	InvddT-GTTCAGAGTTCTACAGTCCGACGATCNNNNNAGC-OH
RT primer	GCCTTGGCACCCGAGAATTCCA
RP1	AATGATACGGCGACCACCGAGATCTACACGTTCAGAGTTCTACAGTCCGA
RPI4	CAAGCAGAAGACGGCATACGAGATTGGTCAGTGACTGGAGTTCCTTGGCACCCGAGAATTCCA
RPI5	CAAGCAGAAGACGGCATACGAGATCACTGTGTGACTGGAGTCCTTGGCACCCGAGAATTCCA
RPI6	CAAGCAGAAGACGGCATACGAGATATTGGCGTGACTGGAGTTCCTTGGCACCCGAGAATTCCA
RPI7	CAAGCAGAAGACGGCATACGAGATGATCTGGTGACTGGAGTTCCTTGGCACCCGAGAATTCCA
RPI12	CAAGCAGAAGACGGCATACGAGATTACAAGGTGACTGGAGTTCCTTGGCACCCGAGAATTCCA
L5Aa	invddT-ACACrGrArCrGrCrUrCrUrUrCrCrGrArUrCrUrNrNrNrUrArArGrC-OH
L5Ab	invddT-ACACrGrArCrGrCrUrCrUrUrCrCrGrArUrCrUrNrNrNrArUrUrArGrC-OH
L5Ac	invddT-ACACrGrArCrGrCrUrCrUrUrCrCrGrArUrCrUrNrNrNrGrCrGrCrArGrC-OH
P5F	AATGATACGGCGACCACCGAGATCTACACTCTTTCCCTACACGACGCTCTTCCGATCT
P3R	CAAGCAGAAGACGGCATACGAGATCCTTGGCACCCGAGAATTCC
4634	AGCTCAAGTACTTTTTCCTGGACATTCGCACCACGCGT
4635	TAAGTACTTGAGCT
4633	Cy5-UGCAUUUCGUCCAGGACGU
4821	Cy5-UGCAUUUCGUCCAGGAC

Bibliography

Albert, B., Léger-Silvestre, I., Normand, C., Ostermaier, M.K., Pérez-Fernández, J., Panov, K.I., Zomerdijk, J.C.B.M., Schultz, P., Gadal, O., 2011. RNA polymerase I-specific subunits promote polymerase clustering to enhance the rRNA gene transcription cycle. J. Cell Biol. 192, 277–293. doi:10.1083/jcb.201006040

Arigo, J.T., Carroll, K.L., Ames, J.M., Corden, J.L., 2006. Regulation of yeast NRD1 expression by premature transcription termination. Mol. Cell 21, 641–651. doi:10.1016/j.molcel.2006.02.005

Artz, S.W., Broach, J.R., 1975. Histidine regulation in Salmonella typhimurium: an activator attenuator model of gene regulation. Proc. Natl. Acad. Sci. USA 72, 3453–3457. doi:10.1073/pnas.72.9.3453

Azouzi, C., Jaafar, M., Dez, C., Abou Merhi, R., Lesne, A., Henras, A.K., Gadal, O., 2021. Coupling between production of ribosomal RNA and maturation: just at the beginning. Front. Mol. Biosci. 8, 778778. doi:10.3389/fmolb.2021.778778

Beltrame, M., Tollervey, D., 1992. Identification and functional analysis of two U3 binding sites on yeast pre-ribosomal RNA. EMBO J. 11, 1531–1542.

Bertrand, K., Korn, L., Lee, F., Platt, T., Squires, C.L., Squires, C., Yanofsky, C., 1975. New features of the regulation of the tryptophan operon. Science 189, 22–26. doi:10.1126/science.1094538

Blattner, C., Jennebach, S., Herzog, F., Mayer, A., Cheung, A.C.M., Witte, G., Lorenzen, K., Hopfner, K.-P., Heck, A.J.R., Aebersold, R., Cramer, P., 2011. Molecular basis of Rrn3-regulated RNA polymerase I initiation and cell growth. Genes Dev. 25, 2093–2105. doi:10.1101/gad.17363311

Briand, J.F., Navarro, F., Gadal, O., Thuriaux, P., 2001. Cross talk between tRNA and rRNA synthesis in Saccharomyces cerevisiae. Mol. Cell. Biol. 21, 189–195. doi:10.1128/MCB.21.1.189-195.2001

Chaker-Margot, M., Barandun, J., Hunziker, M., Klinge, S., 2017. Architecture of the yeast small subunit processome. Science 355. doi:10.1126/science.aal1880

Clarke, A.M., Engel, K.L., Giles, K.E., Petit, C.M., Schneider, D.A., 2018. NETSeq reveals heterogeneous nucleotide incorporation by RNA polymerase I. Proc. Natl. Acad. Sci. USA 115, E11633–E11641. doi:10.1073/pnas.1809421115

Colis, L., Peltonen, K., Sirajuddin, P., Liu, H., Sanders, S., Ernst, G., Barrow, J.C., Laiho, M., 2014. DNA intercalator BMH-21 inhibits RNA polymerase I independent of DNA damage response. Oncotarget 5, 4361–4369. doi:10.18632/oncotarget.2020

Dangkulwanich, M., Ishibashi, T., Liu, S., Kireeva, M.L., Lubkowska, L., Kashlev, M., Bustamante, C.J., 2013. Complete dissection of transcription elongation reveals slow translocation of RNA polymerase II in a linear ratchet mechanism. Elife 2, e00971. doi:10.7554/eLife.00971

Darrière, T., Pilsl, M., Sarthou, M.-K., Chauvier, A., Genty, T., Audibert, S., Dez, C., Léger-Silvestre, I., Normand, C., Henras, A.K., Kwapisz, M., Calvo, O., Fernández-Tornero, C., Tschochner, H., Gadal, O., 2019. Genetic analyses led to the discovery of a super-active mutant of the RNA polymerase I. PLoS Genet. 15, e1008157. doi:10.1371/journal.pgen.1008157

Delan-Forino, C., Schneider, C., Tollervey, D., 2017. Transcriptome-wide analysis of alternative routes for RNA substrates into the exosome complex. PLoS Genet. 13, e1006699. doi:10.1371/journal.pgen.1006699

Dez, C., Houseley, J., Tollervey, D., 2006. Surveillance of nuclear-restricted pre-ribosomes within a subnucleolar region of Saccharomyces cerevisiae. EMBO J. 25, 1534–1546. doi:10.1038/sj.emboj.7601035

Duval, M., Yague-Sanz, C., Turowski, T.W., Petfalski, E., Tollervey, D., Bachand, F., 2023. The conserved RNA-binding protein Seb1 promotes cotranscriptional ribosomal RNA processing by controlling RNA polymerase I progression. Nat. Commun. 14, 3013. doi:10.1038/s41467-023-38826-6

El Hage, A., Koper, M., Kufel, J., Tollervey, D., 2008. Efficient termination of transcription by RNA polymerase I requires the 5' exonuclease Rat1 in yeast. Genes Dev. 22, 1069–1081. doi:10.1101/gad.463708

Engel, C., Neyer, S., Cramer, P., 2018. Distinct mechanisms of transcription initiation by RNA polymerases I and II. Annu. Rev. Biophys. 47, 425–446. doi:10.1146/annurev-biophys-070317-033058

Fetherston, J., Werner, E., Patterson, R., 1984. Processing of the external transcribed spacer of murine rRNA and site of action of actinomycin D. Nucleic Acids Res. 12, 7187–7198. doi:10.1093/nar/12.18.7187

French, S.L., Osheim, Y.N., Cioci, F., Nomura, M., Beyer, A.L., 2003. In exponentially growing Saccharomyces cerevisiae cells, rRNA synthesis is determined by the summed RNA polymerase I loading rate rather than by the number of active genes. Mol. Cell. Biol. 23, 1558–1568. doi:10.1128/MCB.23.5.1558-1568.2003

Gallagher, J.E.G., Dunbar, D.A., Granneman, S., Mitchell, B.M., Osheim, Y., Beyer, A.L., Baserga, S.J., 2004. RNA polymerase I transcription and pre-rRNA processing are linked by specific SSU processome components. Genes Dev. 18, 2506–2517. doi:10.1101/gad.1226604

Granneman, S, Kudla, G., Petfalski, E., Tollervey, D., 2009. Identification of protein binding sites on U3 snoRNA and pre-rRNA by UV cross-linking and high-throughput analysis of cDNAs. Proc Natl Acad Sci U S A 106, 9613–8.

Granneman, Sander, Kudla, G., Petfalski, E., Tollervey, D., 2009. Identification of protein binding sites on U3 snoRNA and pre-rRNA by UV cross-linking and high-throughput analysis of cDNAs. Proc. Natl. Acad. Sci. USA 106, 9613–9618. doi:10.1073/pnas.0901997106

Grummt, I., 2003. Life on a planet of its own: regulation of RNA polymerase I transcription in the nucleolus. Genes Dev. 17, 1691–1702. doi:10.1101/gad.1098503R

Guajardo, R., Sousa, R., 1997. A model for the mechanism of polymerase translocation. J. Mol. Biol. 265, 8–19. doi:10.1006/jmbi.1996.0707

Hadjiolova, K.V., Hadjiolov, A.A., Bachellerie, J.P., 1995. Actinomycin D stimulates the transcription of rRNA minigenes transfected into mouse cells. Implications for the in vivo hypersensitivity of rRNA gene transcription. Eur. J. Biochem. 228, 605–615. doi:10.1111/j.1432-1033.1995.0605m.x

Henras, A.K., Plisson-Chastang, C., O'Donohue, M.-F., Chakraborty, A., Gleizes, P.-E., 2015. An overview of pre-ribosomal RNA processing in eukaryotes. Wiley Interdiscip Rev RNA 6, 225–242. doi:10.1002/wrna.1269

Huffines, A.K., Engel, K.L., French, S.L., Zhang, Y., Viktorovskaya, O.V., Schneider, D.A., 2022. Rate of transcription elongation and sequence-specific pausing by RNA polymerase I directly influence rRNA processing. J. Biol. Chem. 298, 102730. doi:10.1016/j.jbc.2022.102730

Hunziker, M., Barandun, J., Petfalski, E., Tan, D., Delan-Forino, C., Molloy, K.R., Kim, K.H., Dunn-Davies, H., Shi, Y., Chaker-Margot, M., Chait, B.T., Walz, T., Tollervey, D., Klinge, S., 2016. UtpA and UtpB chaperone nascent pre-ribosomal RNA and U3 snoRNA to initiate eukaryotic ribosome assembly. Nat. Commun. 7, 12090. doi:10.1038/ncomms12090

Ibars, E., Codina-Fabra, J., Bellí, G., Casas, C., Tarrés, M., Solé-Soler, R., Lorite, N.P., Ximénez-Embún, P., Muñoz, J., Colomina, N., Torres-Rosell, J., 2023. Ubiquitin proteomics identifies RNA polymerase I as a target of the Smc5/6 complex. Cell Rep. 42, 112463. doi:10.1016/j.celrep.2023.112463

Jacobs, R.Q., Huffines, A.K., Laiho, M., Schneider, D.A., 2022. The small-molecule BMH-21 directly inhibits transcription elongation and DNA occupancy of RNA polymerase I in vivo and in vitro. J. Biol. Chem. 298, 101450. doi:10.1016/j.jbc.2021.101450

Kamieniarz-Gdula, K., Proudfoot, N.J., 2019. Transcriptional control by premature termination: A forgotten mechanism. Trends Genet. 35, 553–564. doi:10.1016/j.tig.2019.05.005

Kim, S., Beltran, B., Irnov, I., Jacobs-Wagner, C., 2019. Long-Distance Cooperative and Antagonistic RNA Polymerase Dynamics via DNA Supercoiling. Cell 179, 106–119.e16. doi:10.1016/j.cell.2019.08.033
Kos, M., Tollervey, D., 2010. Yeast pre-rRNA processing and modification occur cotranscriptionally. Mol. Cell 37, 809–820. doi:10.1016/j.molcel.2010.02.024
Krebs, A.R., Imanci, D., Hoerner, L., Gaidatzis, D., Burger, L., Schübeler, D., 2017. Genome-wide Single-Molecule Footprinting Reveals High RNA Polymerase II Turnover at Paused Promoters. Mol. Cell 67, 411–422.e4. doi:10.1016/j.molcel.2017.06.027
Lesne, A., Victor, J.-M., Bertrand, E., Basyuk, E., Barbi, M., 2018. The role of supercoiling in the motor activity of RNA polymerases. Methods Mol. Biol. 1805, 215–232. doi:10.1007/978-1-4939-8556-2_11
Liu, L.F., Wang, J.C., 1987. Supercoiling of the DNA template during transcription. Proc. Natl. Acad. Sci. USA 84, 7024–7027. doi:10.1073/pnas.84.20.7024
Merkl, P.E., Pilsl, M., Fremter, T., Schwank, K., Engel, C., Längst, G., Milkereit, P., Griesenbeck, J., Tschochner, H., 2020. RNA polymerase I (Pol I) passage through nucleosomes depends on Pol I subunits binding its lobe structure. J. Biol. Chem. 295, 4782–4795. doi:10.1074/jbc.RA119.011827
Moss, T., Langlois, F., Gagnon-Kugler, T., Stefanovsky, V., 2007. A housekeeper with power of attorney: the rRNA genes in ribosome biogenesis. Cell Mol. Life Sci. 64, 29–49. doi:10.1007/s00018-006-6278-1
Noe Gonzalez, M., Blears, D., Svejstrup, J.Q., 2021. Causes and consequences of RNA polymerase II stalling during transcript elongation. Nat. Rev. Mol. Cell Biol. 22, 3–21. doi:10.1038/s41580-020-00308-8
Peltonen, K., Colis, L., Liu, H., Jäämaa, S., Moore, H.M., Enbäck, J., Laakkonen, P., Vaahtokari, A., Jones, R.J., af Hällström, T.M., Laiho, M., 2010. Identification of novel p53 pathway activating small-molecule compounds reveals unexpected similarities with known therapeutic agents. PLoS One 5, e12996. doi:10.1371/journal.pone.0012996
Peltonen, K., Colis, L., Liu, H., Jäämaa, S., Zhang, Z., Af Hällström, T., Moore, H.M., Sirajuddin, P., Laiho, M., 2014a. Small molecule BMH-compounds that inhibit RNA polymerase I and cause nucleolar stress. Mol. Cancer Ther. 13, 2537–2546. doi:10.1158/1535-7163.MCT-14-0256
Peltonen, K., Colis, L., Liu, H., Trivedi, R., Moubarek, M.S., Moore, H.M., Bai, B., Rudek, M.A., Bieberich, C.J., Laiho, M., 2014b. A targeting modality for destruction of RNA polymerase I that possesses anticancer activity. Cancer Cell 25, 77–90. doi:10.1016/j.ccr.2013.12.009
Petfalski, E., Winz, M.-L., Grelewska-Nowotko, K., Turowski, T.W., Tollervey, D., 2025. Multiple mechanisms of termination modulate the dynamics of RNAPI transcription. Cell Rep. 115325. doi:10.1016/j.celrep.2025.115325
Pilsl, M., Crucifix, C., Papai, G., Krupp, F., Steinbauer, R., Griesenbeck, J., Milkereit, P., Tschochner, H., Schultz, P., 2016a. Structure of the initiation-competent RNA polymerase I and its implication for transcription. Nat. Commun. 7, 12126. doi:10.1038/ncomms12126
Pilsl, M., Merkl, P.E., Milkereit, P., Griesenbeck, J., Tschochner, H., 2016b. Analysis of S. cerevisiae RNA Polymerase I Transcription In Vitro. Methods Mol. Biol. 1455, 99–108. doi:10.1007/978-1-4939-3792-9_8
Porrua, O., Libri, D., 2015. Transcription termination and the control of the transcriptome: why, where and how to stop. Nat. Rev. Mol. Cell Biol. 16, 190–202. doi:10.1038/nrm3943
Prescott, E.M., Osheim, Y.N., Jones, H.S., Alen, C.M., Roan, J.G., Reeder, R.H., Beyer, A.L., Proudfoot, N.J., 2004. Transcriptional termination by RNA polymerase I requires the small subunit Rpa12p. Proc. Natl. Acad. Sci. USA 101, 6068–6073. doi:10.1073/pnas.0401393101
Riva, M., Buhler, J.M., Sentenac, A., Fromageot, P., Hawthorne, D.C., 1982. Natural variation in yeast RNA polymerase A. Formation of a mosaic RNA polymerase A in a

meiotic segregant from an interspecific hybrid. J. Biol. Chem. 257, 4570–4577. doi:10.1016/S0021-9258(18)34762-8
Sadian, Y., Baudin, F., Tafur, L., Murciano, B., Wetzel, R., Weis, F., Müller, C.W., 2019. Molecular insight into RNA polymerase I promoter recognition and promoter melting. Nat. Commun. 10, 5543. doi:10.1038/s41467-019-13510-w
Schneider, D.A., Michel, A., Sikes, M.L., Vu, L., Dodd, J.A., Salgia, S., Osheim, Y.N., Beyer, A.L., Nomura, M., 2007. Transcription elongation by RNA polymerase I is linked to efficient rRNA processing and ribosome assembly. Mol. Cell 26, 217–229. doi:10.1016/j.molcel.2007.04.007
Schwank, K., Schmid, C., Fremter, T., Engel, C., Milkereit, P., Griesenbeck, J., Tschochner, H., 2023. Features of yeast RNA polymerase I with special consideration of the lobe binding subunits. Biol. Chem. 404, 979–1002. doi:10.1515/hsz-2023-0184
Schwank, K., Schmid, C., Fremter, T., Milkereit, P., Griesenbeck, J., Tschochner, H., 2022. RNA polymerase I (Pol I) lobe-binding subunit Rpa12.2 promotes RNA cleavage and proofreading. J. Biol. Chem. 298, 101862. doi:10.1016/j.jbc.2022.101862
Scull, C.E., Clarke, A.M., Lucius, A.L., Schneider, D.A., 2020. Downstream sequence-dependent RNA cleavage and pausing by RNA polymerase I. J. Biol. Chem. 295, 1288–1299. doi:10.1074/jbc.RA119.011354
Shcherbik, N., Wang, M., Lapik, Y.R., Srivastava, L., Pestov, D.G., 2010. Polyadenylation and degradation of incomplete RNA polymerase I transcripts in mammalian cells. EMBO Rep. 11, 106–111. doi:10.1038/embor.2009.271
Steinmetz, E.J., Warren, C.L., Kuehner, J.N., Panbehi, B., Ansari, A.Z., Brow, D.A., 2006. Genome-wide distribution of yeast RNA polymerase II and its control by Sen1 helicase. Mol. Cell 24, 735–746. doi:10.1016/j.molcel.2006.10.023
Steurer, B., Janssens, R.C., Geverts, B., Geijer, M.E., Wienholz, F., Theil, A.F., Chang, J., Dealy, S., Pothof, J., van Cappellen, W.A., Houtsmuller, A.B., Marteijn, J.A., 2018. Live-cell analysis of endogenous GFP-RPB1 uncovers rapid turnover of initiating and promoter-paused RNA Polymerase II. Proc. Natl. Acad. Sci. USA 115, E4368–E4376. doi:10.1073/pnas.1717920115
Sun, Q., Zhu, X., Qi, J., An, W., Lan, P., Tan, D., Chen, R., Wang, B., Zheng, S., Zhang, C., Chen, X., Zhang, W., Chen, J., Dong, M.-Q., Ye, K., 2017. Molecular architecture of the 90S small subunit pre-ribosome. Elife 6. doi:10.7554/eLife.22086
Turowski, T.W., Petfalski, E., Goddard, B.D., French, S.L., Helwak, A., Tollervey, D., 2020. Nascent transcript folding plays a major role in determining RNA polymerase elongation rates. Mol. Cell 79, 488–503.e11. doi:10.1016/j.molcel.2020.06.002
Viktorovskaya, O.V., Engel, K.L., French, S.L., Cui, P., Vandeventer, P.J., Pavlovic, E.M., Beyer, A.L., Kaplan, C.D., Schneider, D.A., 2013. Divergent contributions of conserved active site residues to transcription by eukaryotic RNA polymerases I and II. Cell Rep. 4, 974–984. doi:10.1016/j.celrep.2013.07.044
Warner, J.R., 1999. The economics of ribosome biosynthesis in yeast. Trends Biochem. Sci. 24, 437–440. doi:10.1016/s0968-0004(99)01460-7
Wei, T., Najmi, S.M., Liu, H., Peltonen, K., Kucerova, A., Schneider, D.A., Laiho, M., 2018. Small-Molecule Targeting of RNA Polymerase I Activates a Conserved Transcription Elongation Checkpoint. Cell Rep. 23, 404–414. doi:10.1016/j.celrep.2018.03.066
Wery, M., Ruidant, S., Schillewaert, S., Leporé, N., Lafontaine, D.L.J., 2009. The nuclear poly(A) polymerase and Exosome cofactor Trf5 is recruited cotranscriptionally to nucleolar surveillance. RNA 15, 406–419. doi:10.1261/rna.1402709
Woolford, J.L., Baserga, S.J., 2013. Ribosome biogenesis in the yeast Saccharomyces cerevisiae. Genetics 195, 643–681. doi:10.1534/genetics.113.153197
Xie, J., Libri, D., Porrua, O., 2023. Mechanisms of eukaryotic transcription termination at a glance. J. Cell Sci. 136. doi:10.1242/jcs.259873
Zhang, L., Wu, C., Cai, G., Chen, S., Ye, K., 2016. Stepwise and dynamic assembly of the earliest precursors of small ribosomal subunits in yeast. Genes Dev. 30, 718–732. doi:10.1101/gad.274688.115

Figure 1

Azouzi et al. 2025

A

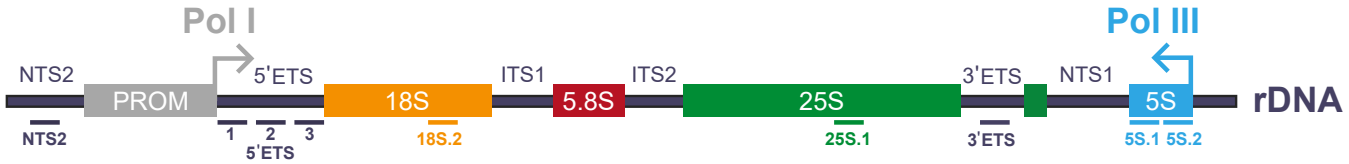

B

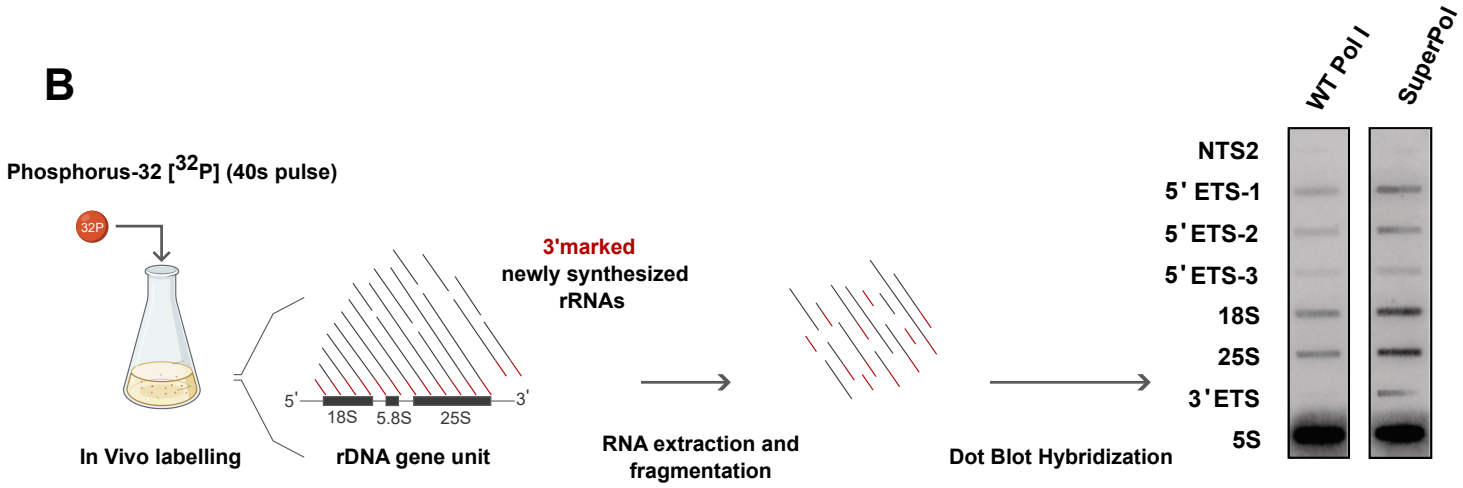

C

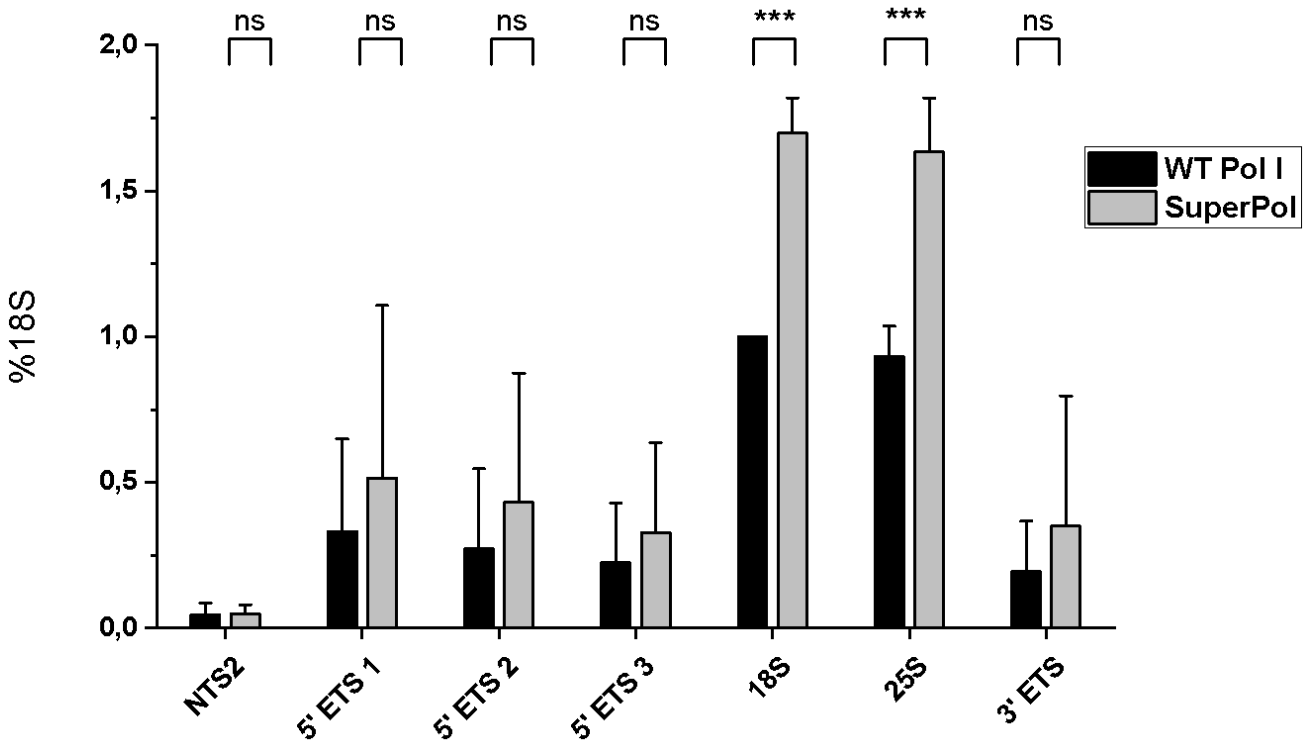

Figure 2

Azouzi et al. 2025

A

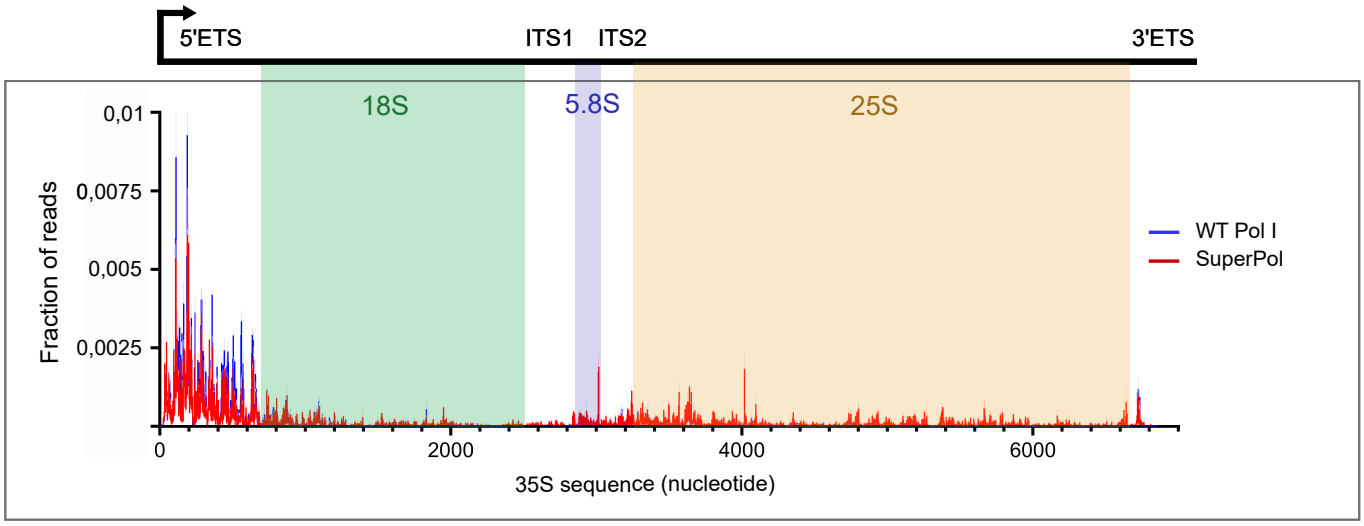

B

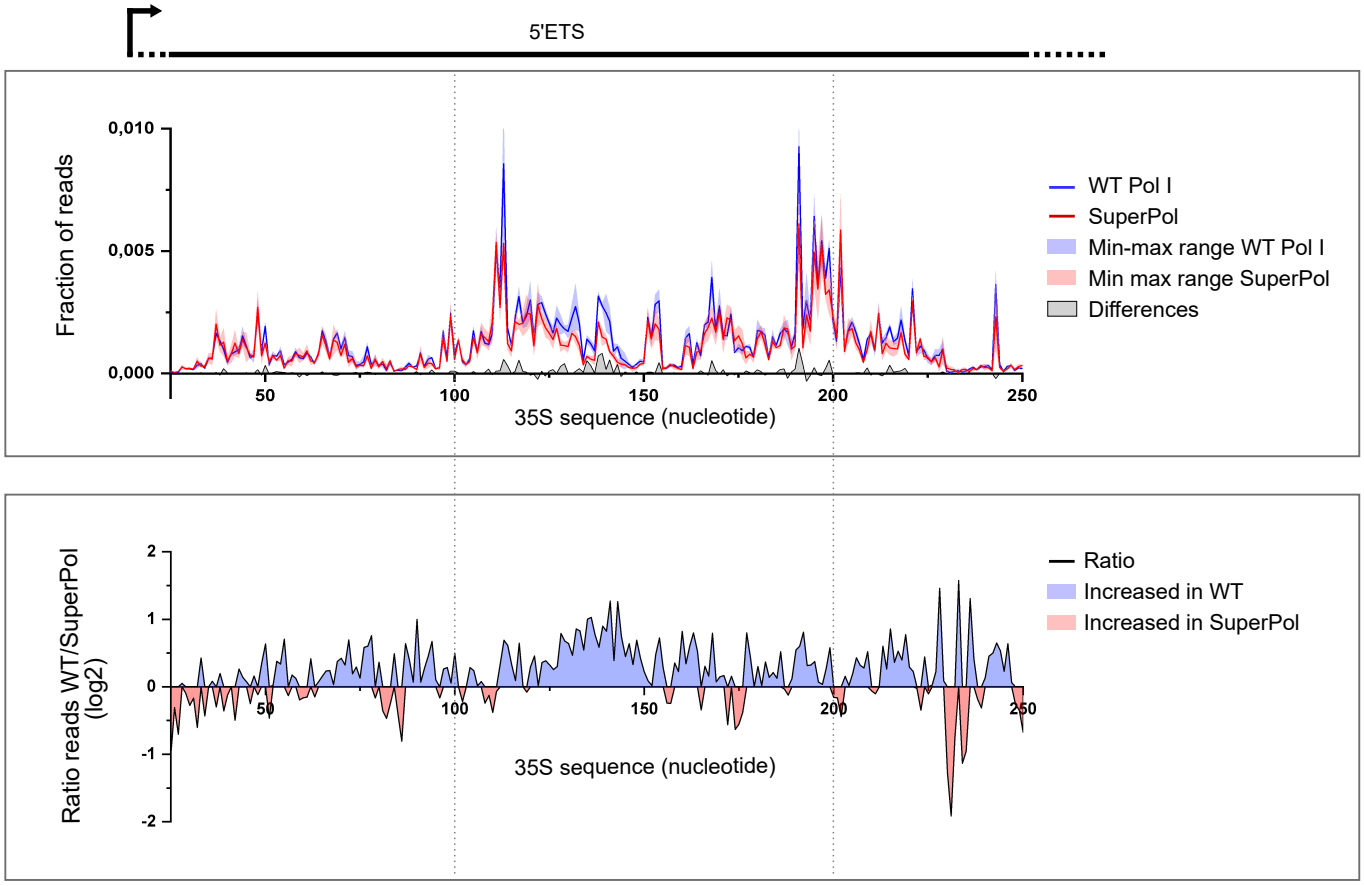

C

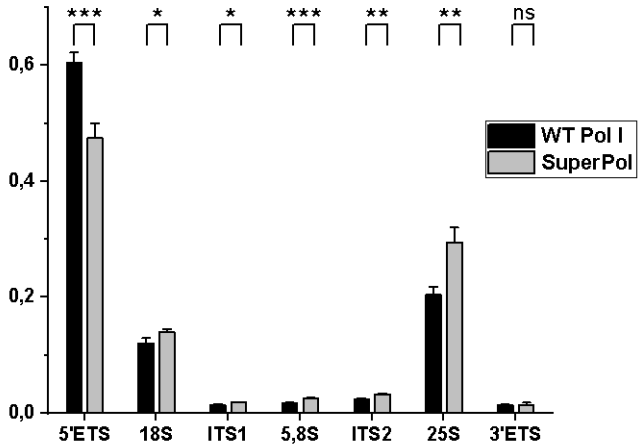

Figure 3

Azouzi et al. 2025

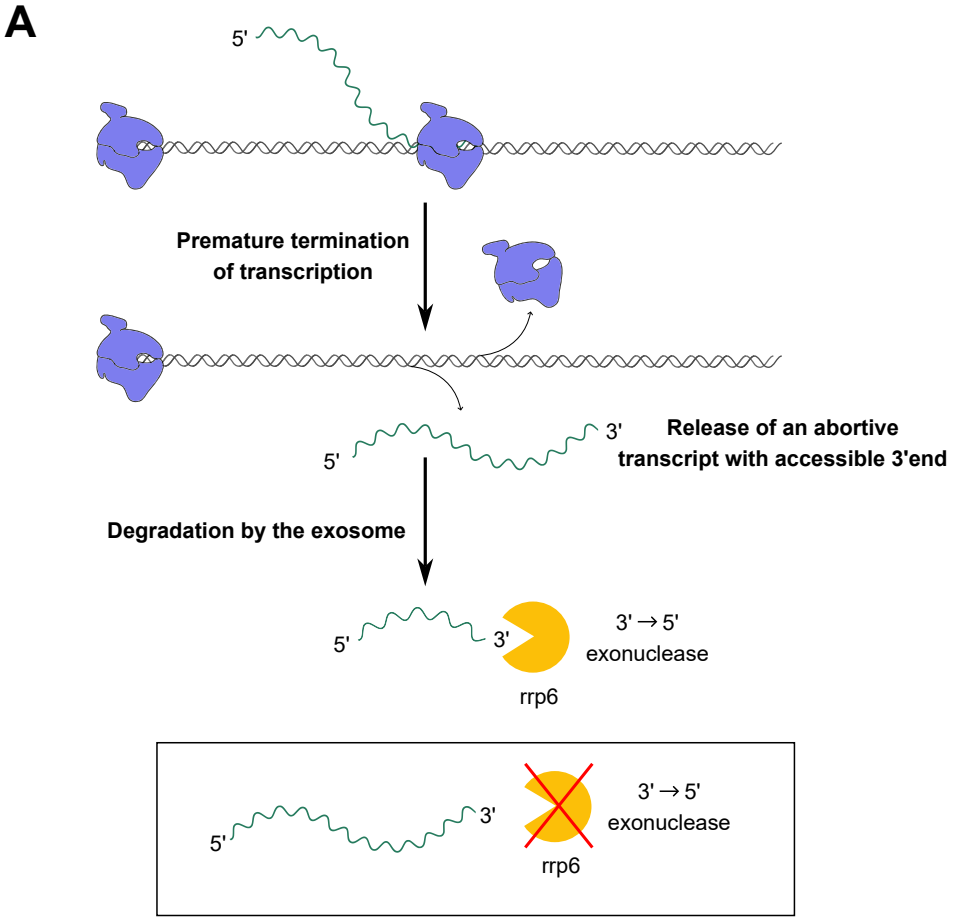

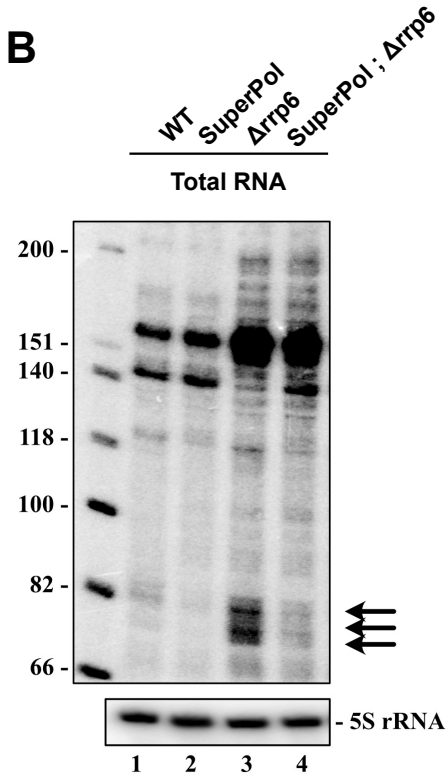

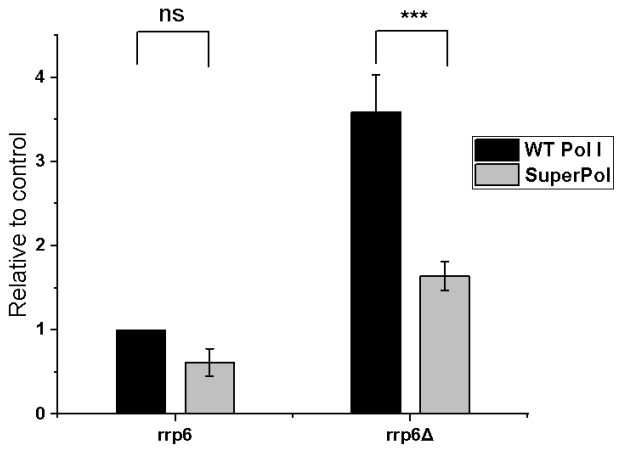

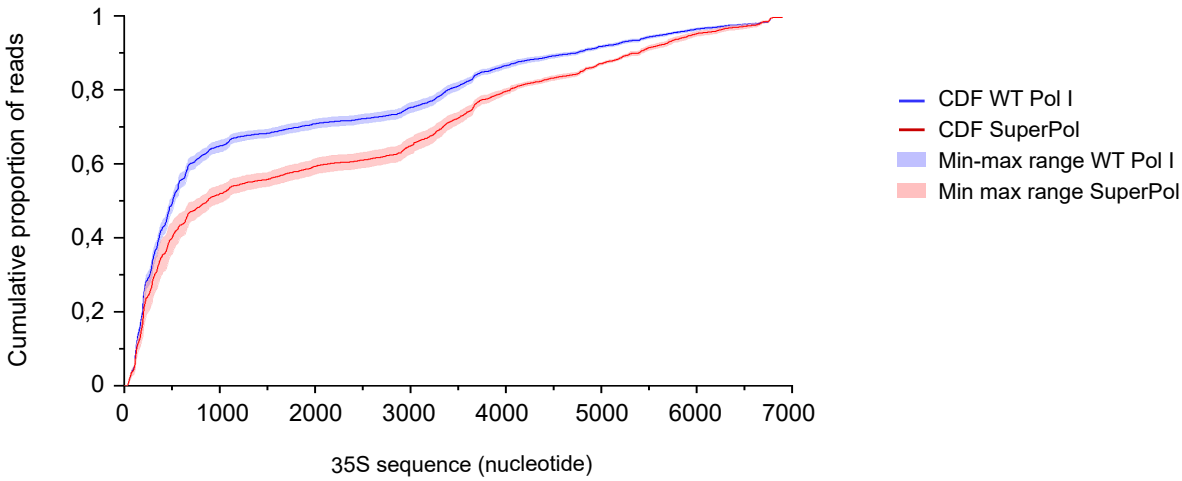

Figure 4

Azouzi et al. 2025

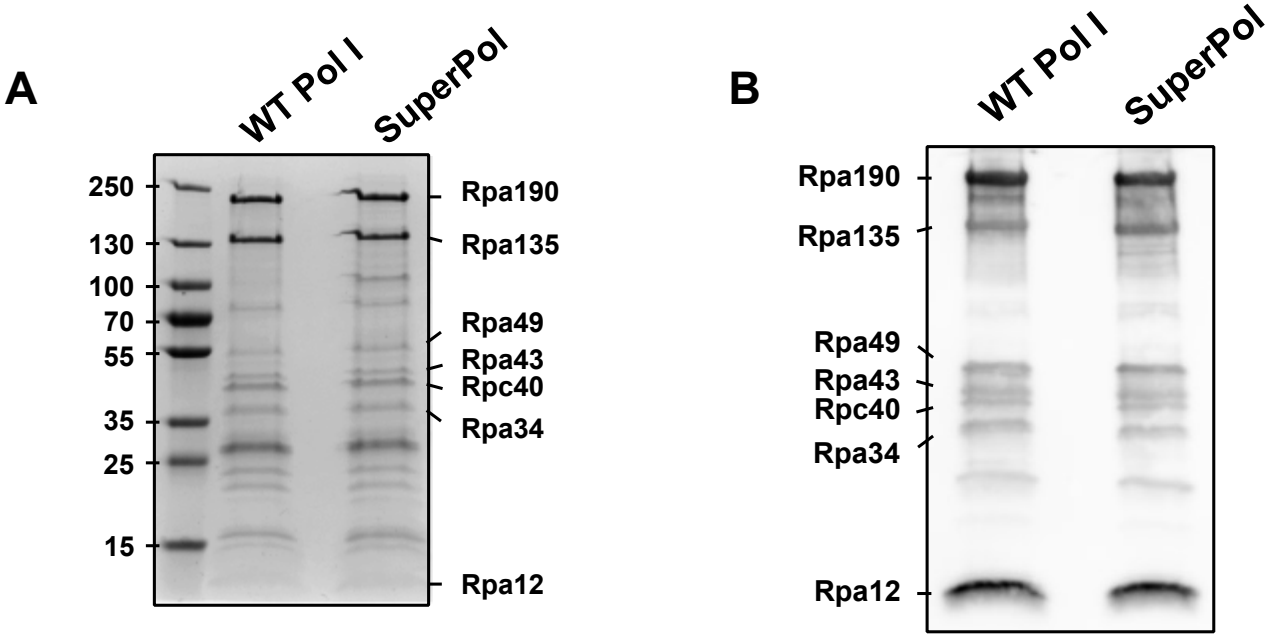

Figure 5

Azouzi et al. 2025

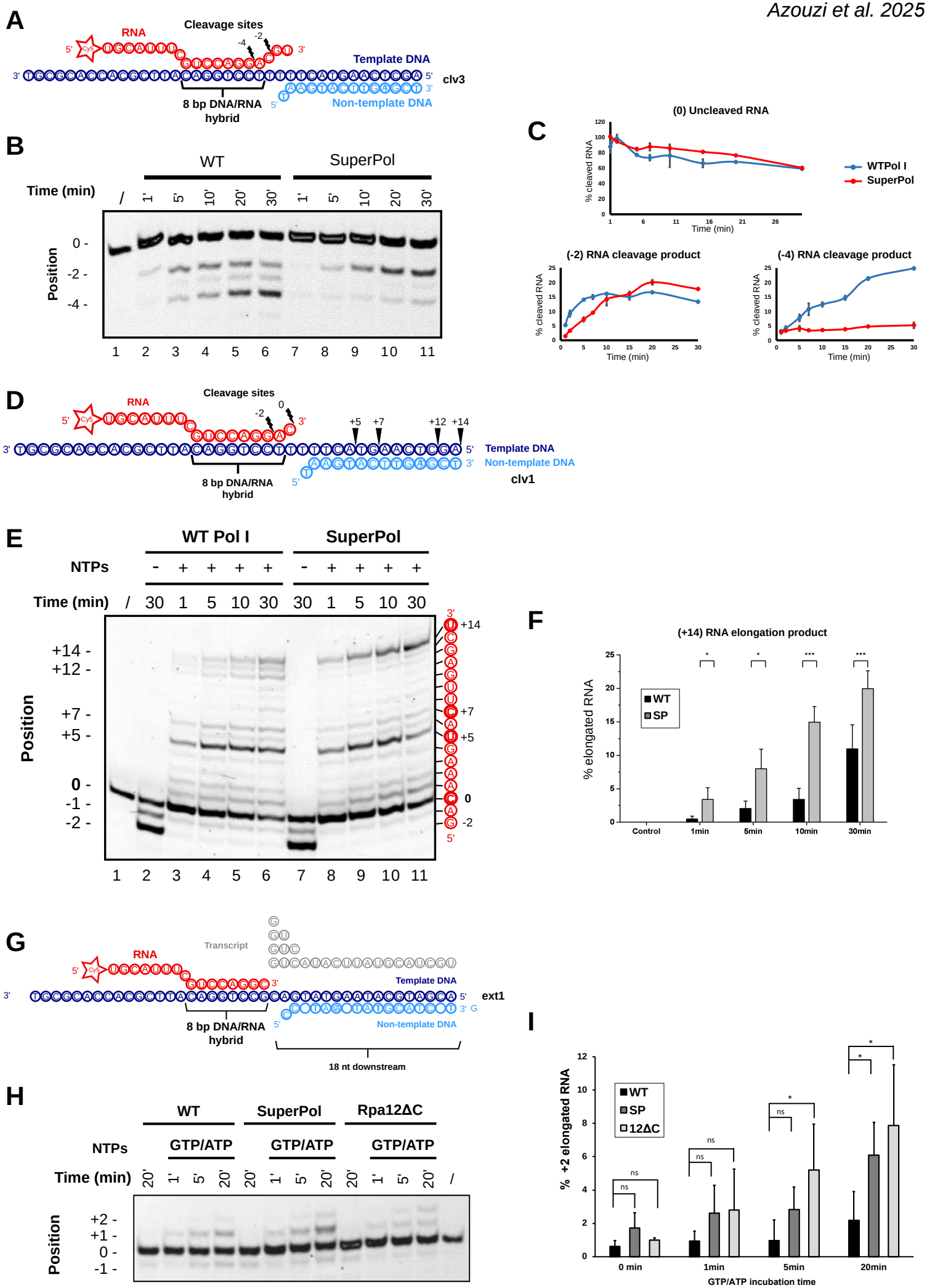

Figure 6

Azouzi et al. 2025

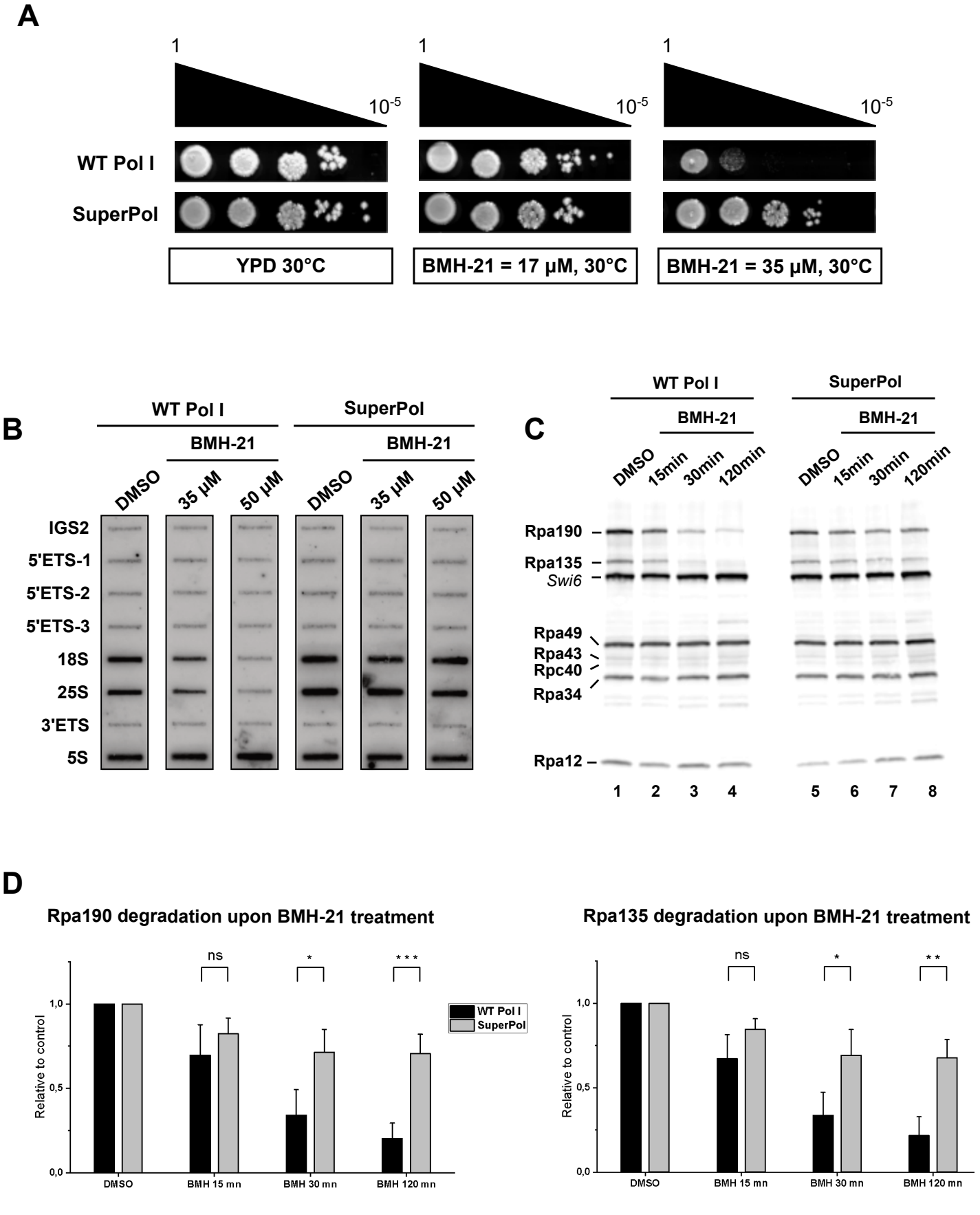

Figure 7

Azouzi et al. 2025

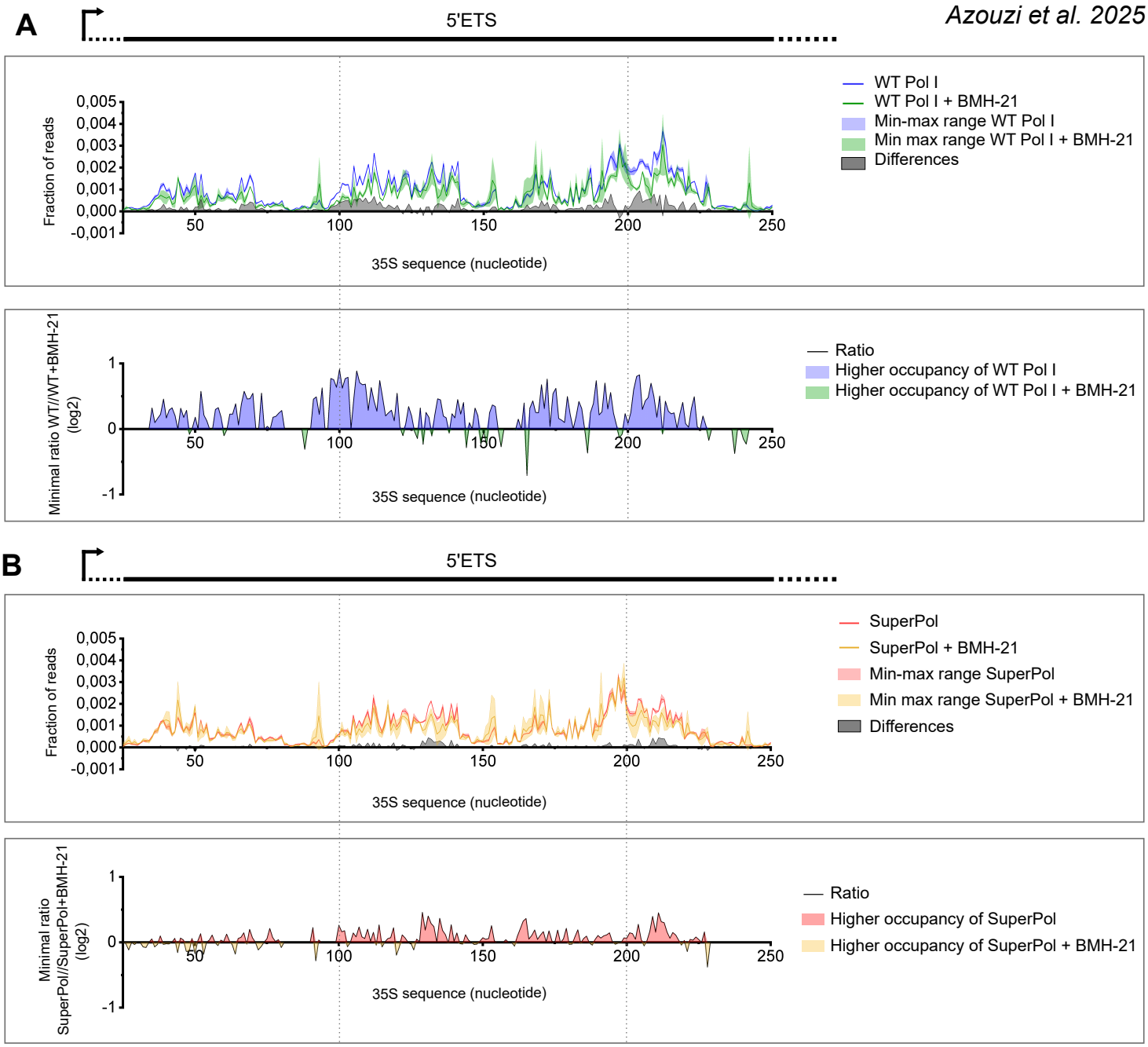

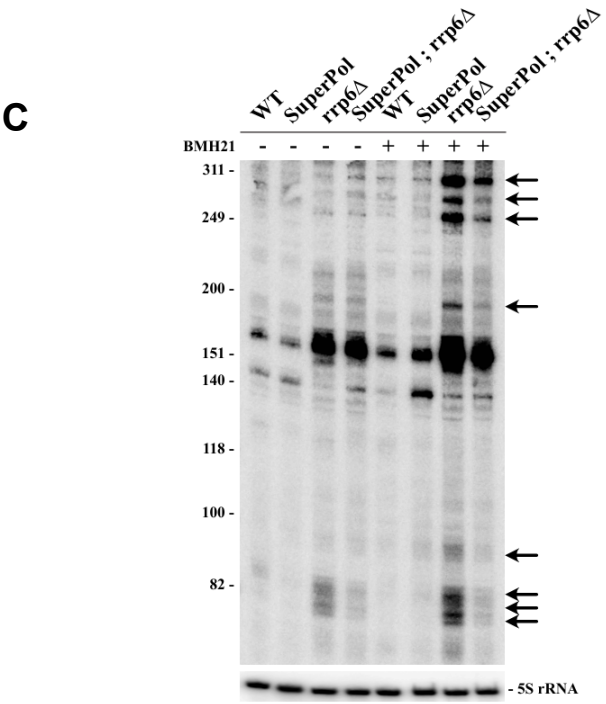

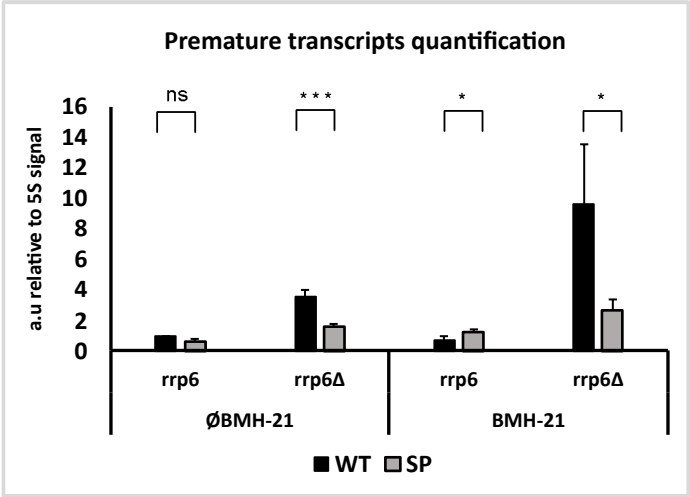

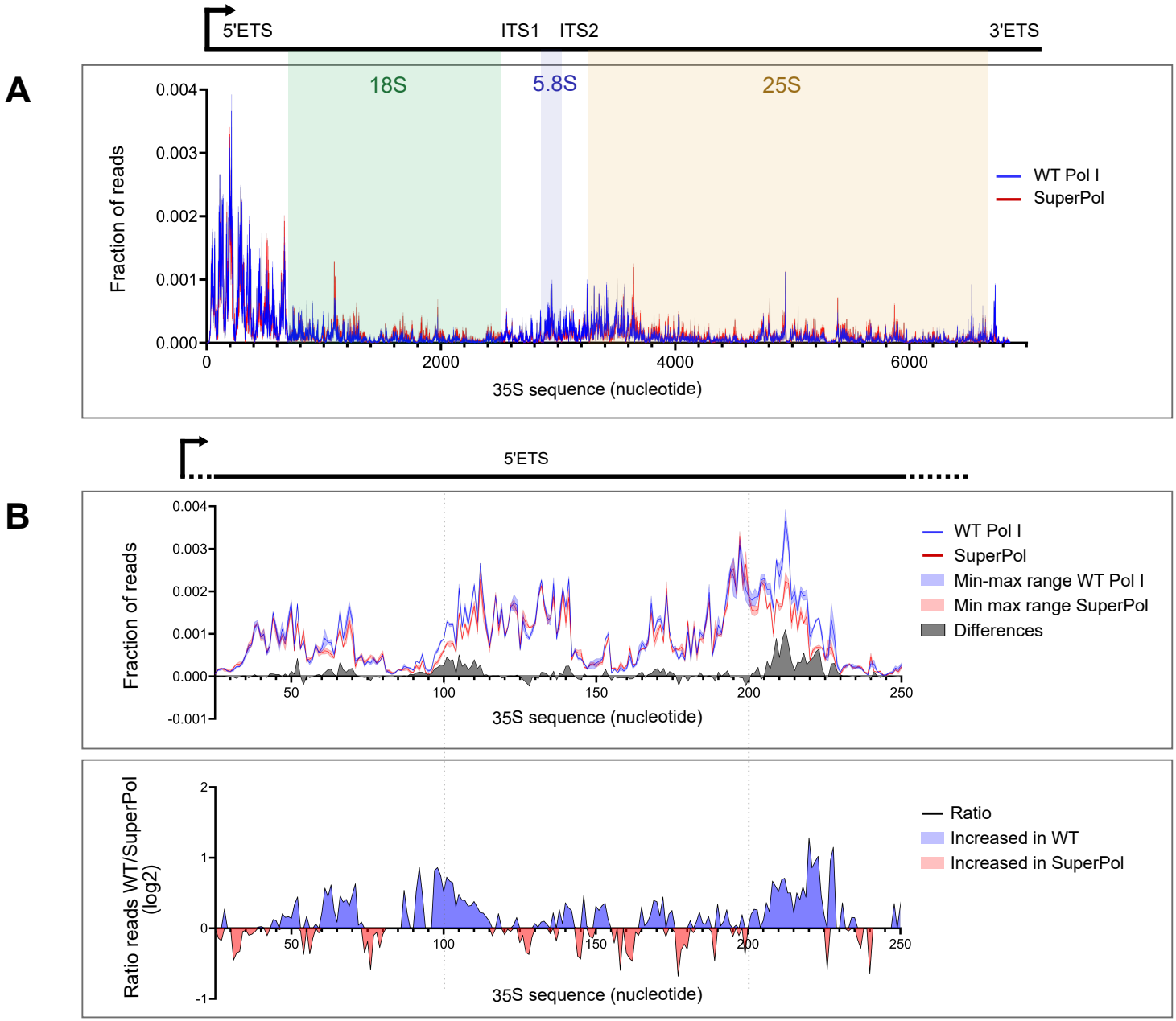

Figure S1: SuperPol displays a lower rate of pause compared to WT Pol I

Figure S1A: CRAC distribution profiles obtained for WT Pol I (Blue line) and SuperPol (Red line). Lines correspond to the mean frequency of reads obtained for two independent experiments. The area of the 35S rDNA gene has been highlighted.

Figure S1B: Zoom in 5'ETS CRAC distribution profiles obtained for WT Pol I (Blue) and SuperPol (Red). In the upper panel, lines correspond to the mean frequency of reads obtained for two independent experiments while the colored area corresponds to the min-max range of the two experiments. The grey area corresponds to the difference between WT Pol I and SuperPol frequency of reads at each position of the gene. This difference has been calculated using the min-max range values giving the lowest difference (white area between blue and red min-max range). The lower panel represents the ratio between WT Pol I and SuperPol, represented in log2. Blue areas correspond to sequences where WT is more accumulated than SuperPol and red areas correspond to the sequences where SuperPol is more accumulated than WT Pol I.

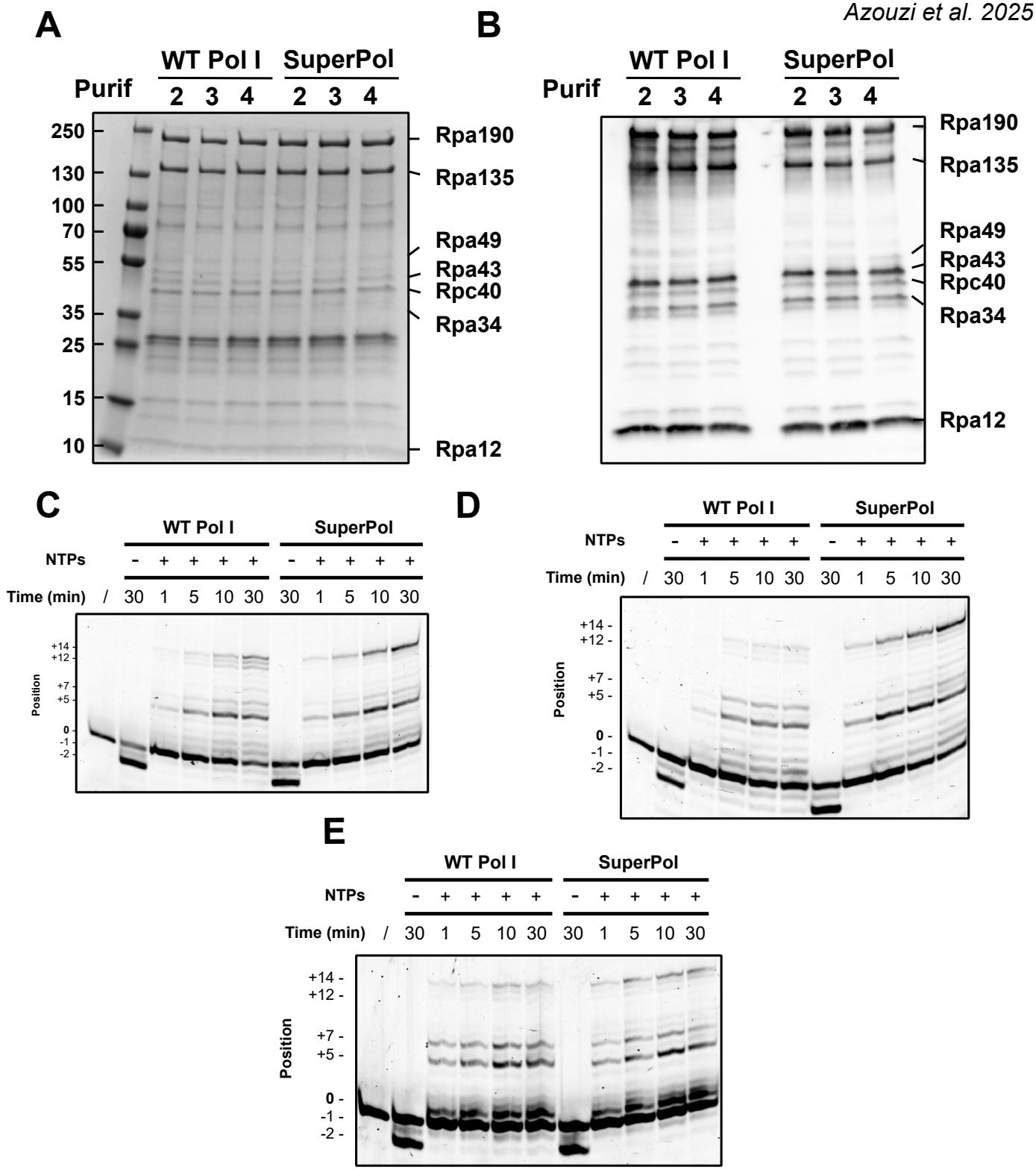

Figure S2: Purification of RNA Pol I and SuperPol and *in vitro* elongation assay

Figure S2A: Tagged WT Pol I and SuperPol were immunopurified respectively from yeast strains #3207 and #3208. Purified fractions from three independant purifications were migrated and separated on 4-12% SDS-PAGE and revealed by Coomassie Blue (see Materials and Methods).

Figure S2B: Tagged WT Pol I and SuperPol were immunopurified respectively from yeast strains #3207 and #3208. Purified fractions from three independant purifications were analyzed by western blot using anti-Pol I antibody (see Materials and Methods).

Figure S2C ; S2D; S2E : Elongation assay from three independant purifications. About 0.15 pmol of either WT Pol I or SuperPol were added to 0.05 pmol cleavage scaffold and incubated with or without nucleotides (200 µM final concentration of each) for the indicated time intervals. Fluorescent transcripts were analyzed on a 20% denaturing polyacrylamide gel. Uncleaved RNAs (0), RNAs shortened by two (-2) nucleotides and elongated RNAs (from +1 to +14) and are indicated with corresponding sequence.